



**HAL**  
open science

**Temporal trends, sources, and relationships between sediment characteristics and polycyclic aromatic hydrocarbons (PAHs) and polychlorinated biphenyls (PCBs) in sediment cores from the major Seine estuary tributary, France**

Thomas Gardes, F. Portet-Koltalo, Maxime Debret, Kevin Humbert, Romain Levailant, Michel Simon, Yoann Copard

► **To cite this version:**

Thomas Gardes, F. Portet-Koltalo, Maxime Debret, Kevin Humbert, Romain Levailant, et al.. Temporal trends, sources, and relationships between sediment characteristics and polycyclic aromatic hydrocarbons (PAHs) and polychlorinated biphenyls (PCBs) in sediment cores from the major Seine estuary tributary, France. *Applied Geochemistry*, 2020, 122, pp.104749. 10.1016/j.apgeochem.2020.104749 . insu-03188432

**HAL Id: insu-03188432**

**<https://insu.hal.science/insu-03188432v1>**

Submitted on 2 Apr 2021

**HAL** is a multi-disciplinary open access archive for the deposit and dissemination of scientific research documents, whether they are published or not. The documents may come from teaching and research institutions in France or abroad, or from public or private research centers.

L'archive ouverte pluridisciplinaire **HAL**, est destinée au dépôt et à la diffusion de documents scientifiques de niveau recherche, publiés ou non, émanant des établissements d'enseignement et de recherche français ou étrangers, des laboratoires publics ou privés.

# Journal Pre-proof



Temporal trends, sources, and relationships between sediment characteristics and polycyclic aromatic hydrocarbons (PAHs) and polychlorinated biphenyls (PCBs) in sediment cores from the major Seine estuary tributary, France

Thomas Gardes, Florence Portet-Koltalo, Maxime Debret, Kevin Humbert, Romain Levailant, Michel Simon, Yoann Copard

PII: S0883-2927(20)30241-9

DOI: <https://doi.org/10.1016/j.apgeochem.2020.104749>

Reference: AG 104749

To appear in: *Applied Geochemistry*

Received Date: 4 June 2020

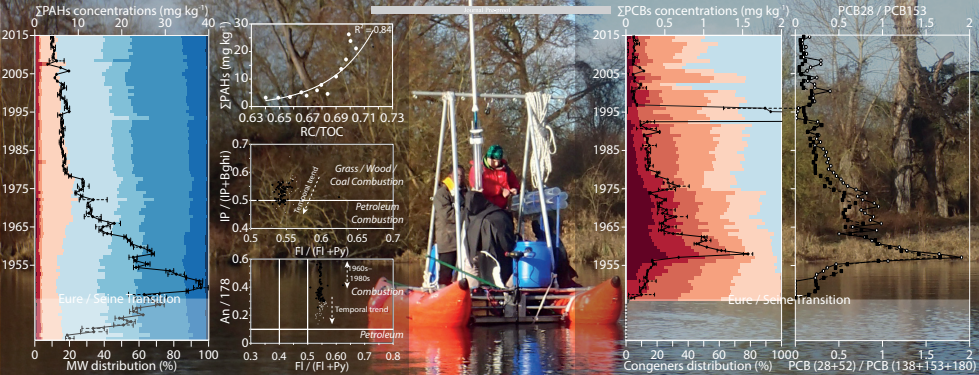
Revised Date: 27 August 2020

Accepted Date: 27 August 2020

Please cite this article as: Gardes, T., Portet-Koltalo, F., Debret, M., Humbert, K., Levailant, R., Simon, M., Copard, Y., Temporal trends, sources, and relationships between sediment characteristics and polycyclic aromatic hydrocarbons (PAHs) and polychlorinated biphenyls (PCBs) in sediment cores from the major Seine estuary tributary, France, *Applied Geochemistry*, <https://doi.org/10.1016/j.apgeochem.2020.104749>.

This is a PDF file of an article that has undergone enhancements after acceptance, such as the addition of a cover page and metadata, and formatting for readability, but it is not yet the definitive version of record. This version will undergo additional copyediting, typesetting and review before it is published in its final form, but we are providing this version to give early visibility of the article. Please note that, during the production process, errors may be discovered which could affect the content, and all legal disclaimers that apply to the journal pertain.

© 2020 Elsevier Ltd. All rights reserved.



1 **Temporal trends, sources, and relationships between sediment**  
2 **characteristics and polycyclic aromatic hydrocarbons (PAHs) and**  
3 **polychlorinated biphenyls (PCBs) in sediment cores from the**  
4 **major Seine estuary tributary, France**

5

6 Thomas Gardes<sup>1,2,\*</sup>, Florence Portet-Koltalo<sup>2</sup>, Maxime Debret<sup>1</sup>, Kevin Humbert<sup>1,2</sup>, Romain  
7 Levailant<sup>1</sup>, Michel Simon<sup>1</sup>, Yoann Copard<sup>1</sup>

8

9 <sup>1</sup>Normandie Univ, Rouen, UNIROUEN, UNICAEN, CNRS, M2C, 76000 Rouen, France.

10 <sup>2</sup>Normandie Univ, Rouen, UMR CNRS 6014 COBRA, 55 Rue Saint Germain, 27000 Evreux, France.

11 \*Corresponding author: thomas.gardes1@univ-rouen.fr

12

13 **Abstract**

14 Temporal trends in polycyclic aromatic hydrocarbons (PAHs) and polychlorinated biphenyls  
15 (PCBs) were reconstructed from sediment cores collected from two ponds downstream of the  
16 Eure River watershed. PAHs exhibited a positive correlation with fine fractions, but mainly  
17 with the refractory organic carbon measured in the sediments, which suggests PAH inputs  
18 from materials largely composed of refractory carbon (e.g. soot). Since the 1940s, PAH  
19 concentrations have ranged between 2.93–38.20 and 2.27–28.20 mg kg<sup>-1</sup>. Based on the  
20 temporal distribution of isomers and diagnostic ratios, the PAHs in the sediments were found  
21 to be predominantly of pyrogenic origin, particularly in the 1940s–1960s, when PAH levels  
22 were particularly high. PCBs also showed an affinity with the fine fraction and with refractory  
23 organic carbon, albeit less so than PAHs. Since the 1940s, PCB concentrations ranged  
24 between 0.02–1.57 and 0.09–1.60 mg kg<sup>-1</sup>. The recorded PCB temporal trends were mainly

25 associated with the production, consumption, and banning of these chemicals in France.  
26 According to the temporal distribution of PCB congeners, high levels in the 1950s–1970s  
27 were linked to "technical mixture" discharges into waterways, which were mainly composed  
28 of "low chlorinated congeners", whereas PCB levels after the 1970s were of atmospheric  
29 origin.

30

### 31 **Keywords**

32 Temporal trends; PAHs; PCBs; sediment cores; refractory organic carbon

33

### 34 **1. Introduction**

35

36 Persistent organic pollutants (POPs) are ubiquitous environmental contaminants that began  
37 to be widely produced and consumed after the Second World War (Bigus et al., 2014). These  
38 organic compounds are not only very stable and therefore difficult to degrade or biodegrade,  
39 but are also often very toxic (Bigus et al., 2014). Additionally, these compounds are generally  
40 highly hydrophobic (Wan et al., 2011; Tobiszewski and Namieśnik, 2012) and therefore tend  
41 to bind to suspended particulate matter (SPM) transported by rivers, thereby accumulating in  
42 aquatic systems (Zennegg et al., 2007).

43 Polycyclic aromatic hydrocarbons (PAHs) are POPs that are released into the environment  
44 both from natural (e.g. fires, volcanoes) and anthropogenic sources (e.g. incomplete  
45 combustion processes, petroleum product leakage), the latter becoming predominant in the  
46 twentieth century (Bigus et al., 2014). PAHs enter aquatic environments via atmospheric  
47 deposition, wastewater discharge from industrial sites, or surface runoff from urban or  
48 industrial areas (Heemken et al., 2000). Petrogenic PAHs (i.e. those derived from petroleum  
49 products or kerogen maturation) are generally emitted directly into aquatic environments,

50 whereas pyrogenic PAHs (i.e. those derived from combustion processes) can be emitted  
51 directly into aquatic environments (e.g. from use or release of coal tar, creosote, manufactured  
52 gas plant wastes and leaking or improperly disposed of used motor oil) or first emitted into  
53 the atmosphere and subsequently enter aquatic environments (Tobiszewski and Namieśnik,  
54 2012). Atmospheric PAH emissions may be associated with particles; alternatively, these  
55 compounds may occur in the gaseous phase when emitted at high temperatures, after which  
56 they may condense onto particles upon cooling (Tobiszewski and Namieśnik, 2012). PAHs  
57 are generally adsorbed onto fine particles but can be transferred from fine to coarser particles  
58 through aggregation over time (Oliveira et al., 2011). PAHs preferentially accumulate in  
59 sediments after entering streams due to their hydrophobicity and generally undergo few or no  
60 changes over many years (Hatzinger and Alexander, 1995; Douglas et al., 1996; Page et al.,  
61 1999). Unlike light PAHs (2–3-ring PAHs), which are more volatile and metabolisable by  
62 microorganisms, heavy PAHs (4–6-ring PAHs) are considered to be relatively stable within  
63 sediment matrices. This accumulation in the sediment can be modulated by the sediment's  
64 composition and characteristics (e.g. particle size, organic carbon ( $C_{org}$ ) content) (Means et  
65 al., 1980; Tobiszewski and Namieśnik, 2012). Notably, PAHs in streams are preferentially  
66 adsorbed onto fine particles (Karickhoff et al., 1979), and thus fine particle sedimentation  
67 leads to the concurrent sedimentation of associated PAHs. PAHs are preferentially adsorbed  
68 onto  $C_{org}$ -rich matrices, and therefore the  $C_{org}$  content in the sediment matrix controls PAHs  
69 behaviour in sediments (Karickhoff et al., 1979; Zhang et al., 2004; Shi et al., 2007).  
70 Moreover, a significant correlation between PAHs and  $C_{org}$  (and soot) levels tends to occur  
71 when PAHs are derived mainly from atmospheric inputs (Tsapakis et al., 2003).

72 Polychlorinated biphenyls (PCBs) are synthetic compounds that were used in various  
73 industrial activities due to their high thermal stability and dielectric properties. Their wide-  
74 spread use, especially after the Second World War, has therefore led to a significant

75 accumulation of these compounds in the environment (Piérard et al., 1996; Breivik et al.,  
76 2002). In France, the use of PCBs was banned in 1987 due to their proven toxicity (Decree  
77 87-59, 1987). The transport of PCBs from terrestrial sources to aquatic environments may  
78 result from direct inputs, following leakage from systems containing them (Abarnou et al.,  
79 1987; Duursma et al., 1989), or from atmospheric deposition following volatilization  
80 (Chevreuil et al., 1989; Quémerais et al., 1994; Granier and Chevreuil, 1997). In the  
81 atmosphere, PCBs are predominantly present in their gaseous phase, after which they bind to  
82 particles through atmospheric deposition (Granier and Chevreuil, 1997). Similar to PAHs,  
83 PCBs are very chemically stable and are only minimally transformed during the  
84 sedimentation process. Due to their lipophilic nature, PCBs accumulate in soils and sediments  
85 by binding to fine particles that are rich in organic matter (OM) and have a high surface-to-  
86 volume ratio (Karickhoff et al., 1979; Gschwend and Wu, 1985). Nevertheless, Piérard et al.  
87 (1996) observed that the affinity of PCBs to OM cannot fully explain the distribution of  
88 sediment PCB concentrations, and that particle size is the major factor explaining their  
89 distribution. Specifically, PCBs generally accumulate in fine particles, especially highly  
90 chlorinated PCBs, which have a particular affinity for fine fractions ( $< 63 \mu\text{m}$ ), whereas low  
91 chlorinated PCBs have more affinity for coarse fractions ( $> 63 \mu\text{m}$ ) (Piérard et al., 1996;  
92 Salvadó et al., 2013).

93 Based on sediment cores collected in accumulation areas (e.g. dams, floodplains, ponds), the  
94 temporal trends of PAHs and PCBs can be reconstructed (Sanders et al., 1992; Van Metre et  
95 al., 1997; Budzinski et al., 1997; Bertrand et al., 2015; Cai et al., 2016). Thus, it is possible to  
96 reconstruct the contamination trends of a watershed, generally in relation to the intensification  
97 of significant anthropogenic activities since the industrial revolution (i.e. over the past ~150  
98 years). Sediment deposits typically provide insights into multiple contaminant sources and  
99 therefore it is necessary to discriminate sources by analysing the distribution of PAH isomers

100 and PCB congeners over time via measured-concentration diagnostic ratios (Budzinski et al.,  
101 1997; Yunker et al., 2002; Francú et al., 2010; Cai et al., 2016).

102 The Seine River watershed is among the most heavily impacted watersheds in Europe  
103 (Meybeck, 2002) and therefore the Seine River has been afflicted with substantial heavy  
104 metal (Le Cloarec et al., 2011) and organic contaminant (Lorgeoux et al., 2016) burdens.  
105 Although many studies have examined POP contaminations in water, SPM, and sediments in  
106 the Seine River (Chevreuil et al., 1990; Chevreuil and Granier, 1991; Chevreuil et al., 1998;  
107 Blanchard et al., 2007; Lorgeoux et al., 2016), few studies have focused on its tributaries (e.g.  
108 the Marne River) (Chevreuil and Granier, 1991; Ollivon et al., 2002) or the Seine estuary  
109 (Abarnou et al., 1987; Marchand, 1989; Van Metre et al., 2008). Regarding the latter, only the  
110 works of Van Metre et al. (2008) have focused on sedimentary archives downstream of the  
111 estuary; however, contamination sources in this area appear to be intra-estuarine.

112 The main Seine estuary tributary is the Eure River. Moreover, the Eure River watershed was  
113 recently found to carry significant heavy metal burdens since the 1940s, which may have  
114 impacted the sediment quality of the Seine estuary (Gardes et al., 2020a, 2020b). Therefore,  
115 this study aimed to establish a link between sediment deposit characteristics and POPs, as  
116 well as to reconstruct the temporal trends in PAHs and PCBs accumulation based on sediment  
117 cores collected downstream of the Eure River watershed. The distribution of some PAH  
118 isomers and PCB congeners was also studied to determine contaminant sources and the  
119 evolution of these sources over time.

120

## 121 **2. Materials and Methods**

122

### 123 2.1. Description of core sites

124



125 The Eure River (watershed: 6017 km<sup>2</sup>; mean annual flow:  $22.13 \pm 6.69 \text{ m}^3 \text{ s}^{-1}$ ) is one of the  
126 largest tributaries of the Seine River (i.e. only surpassed by the Yonne, Marne, and Oise  
127 rivers) and the main contributing river in its estuarine section (Fig. 1A). Les Damps Pond  
128 (average depth: 50 cm; area: < 1 ha) and Martot Pond (area: ~7 ha) are located approximately  
129 10 km and less than 1 km upstream of the Eure River outlet, respectively (Fig. 1B). Unlike  
130 Les Damps Pond, Martot Pond is affected by the Seine estuary during tidal flows through the  
131 Eure River outlet. Moreover, Martot Dam, located 200 m downstream of the Martot Pond,  
132 prevented tidal flows (for tidal coefficients lower than 70) until its removal in October 2017.  
133 Sediment cores were collected using a UWITEC® gravity core and 90 mm diameter PVC  
134 tubes. The water-sediment interface was preserved for each coring. For Les Damps Pond,  
135 sediment cores DAM15-02 and DAM17-02 were collected in January 2015 and January 2017,  
136 respectively (Fig. 1C; Table 1). For Martot Pond, sediment cores MAR15-01 and MAR16-02  
137 were collected in January 2015 and February 2016, respectively (Fig. 1D; Table 1). This study  
138 was conducted on sediment cores from two accumulation zones to (i) ensure that the recorded  
139 temporal trends were representative of a global signal and (ii) determine whether  
140 sedimentation in Martot pond was impacted by inputs from the Seine estuary.

141

## 142 2.2. Grain size and total organic carbon analysis

143

144 Grain size distribution was measured by laser diffraction (LS 13320 Particle Size Analyser  
145 Beckman Coulter™). The measurements were conducted every cm by integrating 1 cm on the  
146 MAR15-01 and DAM15-02 cores.

147 Sediment cores were analysed using Rock-Eval 6 (RE6) pyrolysis ("Turbo" model RE6  
148 pyrolyzer; ISTO laboratory, University of Orléans; see details in Copard et al. (2006)). Total  
149 organic carbon content (TOC; %) was measured and OM quality was determined by

150 measuring the hydrogen index (HI; i.e. indicator of the hydrogen richness; mg HC g<sup>-1</sup> TOC)  
151 and oxygen (OI; indicator of the degree of oxidation of the OM; mg O<sub>2</sub> g<sup>-1</sup> TOC) (Lafargue et  
152 al., 1998; Carrie et al., 2012). Additionally, the residual carbon content (RC; %), which  
153 corresponds to the refractory C<sub>org</sub> (obtained during the oxidation phase), was also measured  
154 (Lafargue et al., 1998). The measurements were conducted on the MAR15-01 and DAM17-02  
155 cores at 1- and 2-cm intervals, respectively.

156

### 157 2.3. Particulate PAHs/PCBs extraction, analysis and quality control and assurance

158

159 Each sediment core segment was freeze-dried, crushed, and stored at -25 °C. Afterwards,  
160 PAHs and PCBs extractions were performed using microwave-assisted extraction (MAE)  
161 (MarsX, CEM Corporation). Approximately 2–3 g of sub-samples were taken from each dried  
162 portion of the sediment cores and spiked with 15 µL of surrogate standards (perdeuterated  
163 fluoranthene and benzo[*a*]pyrene, and PCB156 at 100 mg L<sup>-1</sup>). Each sub-sample was  
164 extracted in duplicate with 40 mL of a toluene:acetone 1:1 (v:v) mixture at 130 °C for 30 min  
165 (1,200 W). The extracts were filtered through 0.2-µm PTFE filters, evaporated, and  
166 reconstituted in 1.5 mL toluene. Each extract (990 µL) was mixed with 10 µL of two internal  
167 standards (perdeuterated phenanthrene and perylene at 100 mg L<sup>-1</sup>), after which 1 µL of the  
168 resulting mixture was injected (splitless mode, 285 °C) into a gas chromatographer (6850  
169 series, Agilent), coupled with a mass spectrometer (5975C series). The separation was  
170 performed using a 60 m × 0.25 mm i.d. DB-5MS capillary column (0.25 µm film thickness;  
171 J&W Scientific), with helium as the carrier gas (1.4 mL min<sup>-1</sup>). The oven temperature was  
172 programmed at 60 °C for 1.2 min, increased to 190 °C (40 °C min<sup>-1</sup>) and then to 305 °C (6 °C  
173 min<sup>-1</sup>). The MS detector operated at 70 eV. Quantification was based on selected ion  
174 monitoring to improve sensitivity. The extraction method was validated using a certified

175 reference sediment (CNS391, Sigma-Aldrich). Mean recoveries (n=5) were in the 86.3–  
176 125.8% range for the 16 priority PAHs (US EPA, 2015) and in the 81.9–113.6% range for the  
177 6 studied PCBs. Table 2 summarizes all PAHs and PCBs studied herein.

178

### 179 3. Results and discussion

180

#### 181 3.1. Sedimentology characteristics of the sediment cores

182

183 The sediment deposits in Martot Pond are characterised by two sedimentary facies, as  
184 previously described by Gardes et al. (2020b). The “Seine Unit” facies corresponds to  
185 sediment deposits from the Seine River watershed until the early 1940s, when Martot Pond  
186 was connected to the Seine channel. The grain size distribution exhibited a low  $D_{50}$  ( $D_{50} =$   
187  $13.8 \pm 7.0 \mu\text{m}$ ), the TOC content ( $\text{TOC}_{\text{mean}} = 1.75 \pm 0.33\%$ ) was low, HI ( $\text{HI}_{\text{mean}} = 147 \pm 24$   
188  $\text{mg HC g}^{-1} \text{TOC}$ ) was constant, OI ( $\text{OI}_{\text{mean}} = 260 \pm 35 \text{ mg O}_2 \text{ g}^{-1} \text{TOC}$ ) increased to 103.5 cm  
189 followed by a decrease, and the average RC/TOC was  $0.76 \pm 0.01$ . The “Eure Unit” facies, for  
190 which an age model has been established, corresponds to the Eure River inputs since the  
191 1940s, with a sedimentation rate of  $12.73 \pm 2.2 \text{ mm y}^{-1}$  (Gardes et al., 2020b). For this facies,  
192 the grain size distribution was centred around a  $D_{50}$  of  $33.9 \pm 7.8 \mu\text{m}$  and the TOC content  
193 ( $\text{TOC}_{\text{mean}} = 3.88 \pm 1.49\%$ ) increased towards the surface, with high contents ( $\text{TOC} = 8.26 \pm$   
194  $0.19\%$ ) in the 9–12 cm range. Unlike OI ( $\text{OI}_{\text{mean}} = 150 \pm 17 \text{ mg O}_2 \text{ g}^{-1} \text{TOC}$ ), HI ( $\text{HI}_{\text{mean}} =$   
195  $279 \pm 23 \text{ mg HC g}^{-1} \text{TOC}$ ) increased from the transition between the two facies. RC/TOC  
196 ( $\text{RC/TOC}_{\text{mean}} = 0.70 \pm 0.02$ ) decreased from the interface between the two facies and  
197 continued to decrease towards the surface (Fig. 2).

198 The sediment deposits in Les Damps Pond are also referred to as the “Eure Unit” facies, and  
199 correspond to the Eure River inputs since the 1940s, with a sedimentation rate of  $12.2 \text{ mm y}^{-1}$

200 (Gardes et al., 2020b). These sediment deposits are characterised by a grain size distribution  
201 centred around a  $D_{50}$  of  $29.5 \pm 6.7 \mu\text{m}$ , comparable to that measured for the "Eure Unit" facies  
202 in Martot Pond, with a constant TOC content ( $\text{TOC}_{\text{mean}} = 5.36 \pm 0.47\%$ ) that is slightly higher  
203 than that of Martot Pond. HI ( $\text{HI}_{\text{mean}} = 302 \pm 23 \text{ mg HC g}^{-1} \text{ TOC}$ ) and OI ( $\text{OI}_{\text{mean}} = 145 \pm 10$   
204  $\text{ mg O}_2 \text{ g}^{-1} \text{ TOC}$ ) showed a slight increase towards the surface. RC/TOC ( $\text{RC/TOC}_{\text{mean}} = 0.68$   
205  $\pm 0.02$ ) decreased towards the surface, similar to our observations in Martot Pond (Fig. 2).

206 In Martot and Les Damps ponds, HI and OI for the "Eure Unit" facies suggested a mix  
207 aquatic/terrestrial origin (Gardes et al., 2020b) and the mean RC/TOC values were similar and  
208 comparable to those measured in the surface sediments of other European rivers (e.g. the  
209 Danube, Elbe, Ebro, and Meuse rivers; Poot et al. (2014)). For both ponds, the sedimentation  
210 rates were found to be high (e.g.  $\geq 10 \text{ mm y}^{-1}$ ), and therefore it is unlikely that the sediments  
211 are affected by early diagenesis processes (Van Metre et al., 1997; Callender, 2000).

212

### 213 3.2. Relationships between PAHs, PCBs, and sediment characteristics

214

215 In Martot Pond, PAH and PCB concentrations were determined on the MAR16-02 core  
216 (Sections 3.3 and 3.4), whereas the grain size distribution and TOC contents (and associated  
217 OM parameters) were determined on the MAR15-01 core (Section 3.1). In Les Damps Pond,  
218 PAH and PCB concentrations were determined on the DAM17-02 core (Sections 3.3 and 3.4),  
219 as well as TOC contents, whereas grain size distribution was determined on the DAM15-02  
220 core. Therefore, the measurements were averaged over decades for each core to determine the  
221 correlations between PAH and PCB contents and grain size or OM in both ponds.

222 In both ponds, total PAH concentrations ( $\sum\text{PAHs}$ ) and light (2-3-ring) or heavy (4-6-ring)  
223 PAHs exhibited weak positive correlations with the clay fraction ( $< 2 \mu\text{m}$ ) ( $0.28 < R < 0.39$   
224 and  $0.23 < R < 0.33$  for Martot and Les Damps ponds, respectively) (Fig. 3A). In Les Damps

225 Pond, PAHs showed strong positive correlations with the fine fraction ( $< 63 \mu\text{m}$ ), particularly  
226 with the silt fraction ( $2\text{--}63 \mu\text{m}$ ) ( $0.74 < R < 0.8$ ). Finally, PAHs showed negative correlations  
227 with the coarse fraction ( $> 63 \mu\text{m}$ ) in Les Damps Pond ( $-0.69 < R < -0.75$ ). Therefore, PAHs  
228 tend to bind more strongly to the fine fraction (Karickhoff et al., 1979; Fernandes et al., 1997;  
229 Shi et al., 2007), and more specifically to the silt fraction in Les Damps Pond, as previously  
230 demonstrated elsewhere by Ab Razak et al. (1996) with sediment cores from the Kinnickinnic  
231 River (US) and Burgess et al. (2001) with surface sediments collected in the Narragansett Bay  
232 estuary (US), or to the clay fraction in the Martot Pond, as also reported by Zhang et al.  
233 (2004) with surficial sediments of Deep Bay (China).

234 PAHs were negatively correlated with (i) the TOC in Martot Pond ( $-0.63 < R < -0.80$ ), (ii)  
235 HI ( $-0.48 < R < -0.77$  and  $-0.89 < R < -0.93$  for Martot and Les Damps ponds, respectively)  
236 and OI ( $-0.27 < R < -0.76$  and  $-0.55 < R < -0.6$  for Martot and Les Damps ponds,  
237 respectively). However,  $\Sigma\text{PAHs}$  showed strong positive correlations with the RC/TOC ratio  
238 ( $R = 0.86$  and  $R = 0.95$  for Martot and Les Damps ponds, respectively) (Fig. 3A).

239 The distribution of PAHs in the sediment is thus partly controlled by the presence of fine  
240 particles, but more predominantly controlled by the presence of refractory  $C_{\text{org}}$ . Moreover, in  
241 Martot Pond, the correlation between PAHs and RC/TOC tended to increase with the molar  
242 mass of the PAHs (from  $R = 0.53$  for 2-ring PAHs to  $R = 0.91$  for 6-ring PAHs). However,  
243 this trend was not observed in Les Damps Pond, where the correlation between PAHs and  
244 RC/TOC was very strong regardless of molar mass ( $0.91 < R < 0.95$ ). A correlation between  
245 the PAHs and the proportion of refractory  $C_{\text{org}}$  (i.e. RC/TOC) would thus demonstrate that  
246 part of the PAHs was bound to refractory carbonaceous compounds. Such an affinity has been  
247 previously identified, albeit from the RC (%) (Poot et al., 2014) and not from the RC/TOC  
248 ratio. Additionally, PAHs showed a correlation with the RC/TOC ratio regardless of ring  
249 number, but only in Les Damps Pond (Fig. 3B). However, this trend remains to be confirmed,

250 especially to determine whether the proportion of refractory  $C_{org}$  is indeed the limiting factor,  
251 as suggested by the observed correlations.

252 PCBs showed positive correlations with the fine fraction (clay + silt) ( $0.20 < R < 0.56$  and  
253  $0.16 < R < 0.71$  for Martot and Les Damps ponds, respectively) and negative correlations with  
254 the coarse fraction ( $-0.20 < R < -0.56$  and  $-0.16 < R < -0.71$  for Martot and Les Damps ponds,  
255 respectively) (Fig. 3A). A positive correlation of PCBs with the fine fraction suggests an  
256 affinity of PCBs for fine particles, but no clear trends (e.g. as a function of PCB chlorination  
257 degree) were evident. Moreover, Piérard et al. (1996) demonstrated that low-chlorinated  
258 PCBs showed an affinity for the coarse fraction, which was not observed in our study.

259 PCBs also showed negative correlations with TOC in Martot Pond ( $-0.69 < R < -0.79$ ), as  
260 well as with HI ( $-0.35 < R < -0.79$  and  $-0.27 < R < -0.92$  for Martot and Les Damps ponds,  
261 respectively) and OI ( $-0.37 < R < -0.72$  and  $-0.15 < R < -0.79$  for Martot and Les Damps  
262 ponds, respectively) (Fig. 3A). However, the  $\sum$ PCBs showed positive correlations with the  
263 RC/TOC ratio ( $R = 0.68$  and  $R = 0.79$  for Martot and Les Damps ponds, respectively). The  
264 distribution of PCBs in sediments is thus partly controlled by fine particles and refractory  
265  $C_{org}$ , but the affinity between PCBs and refractory  $C_{org}$  is generally less marked than for  
266 PAHs.

267

### 268 3.3. PAHs in sediment cores

269

#### 270 3.3.1. General PAH trends in sediment cores

271 Total PAH concentrations were measured for the MAR16-02 and DAM17-02 cores (Fig. 4)  
272 For the MAR16-02 core Seine Unit (78–90 cm), PAH concentrations ranged from 7.43 to  
273  $28.8 \text{ mg kg}^{-1}$  ( $\text{PAH}_{\text{mean}} = 19.9 \pm 1.47 \text{ mg kg}^{-1}$ ) and showed a constant increase towards the  
274 Eure Unit. For the Eure Unit of the MAR16-02 and DAM17-02 cores, concentrations ranged

275 between 2.93–38.20 mg kg<sup>-1</sup> (PAH<sub>mean</sub> = 12.70 ± 0.51 mg kg<sup>-1</sup>) and 2.27–28.20 mg kg<sup>-1</sup>  
276 (PAH<sub>mean</sub> = 11.10 ± 0.89 mg kg<sup>-1</sup>), respectively. For the MAR16-02 core, the upward trend  
277 measured in the Seine Unit continued after the transition to the Eure Unit, reaching a peak of  
278 38.20 ± 1.70 mg kg<sup>-1</sup> in the late 1940s. For the DAM17-02 core, high concentrations were  
279 measured during the 1940s–1950s and two peaks were observed at 28.20 ± 2.44 and 26.10 ±  
280 0.58 mg kg<sup>-1</sup>. PAH concentrations began to decrease from the 1960s to the early 1980s. For  
281 the most recent deposition (post-1980s), concentrations were largely constant, ranging  
282 between 4 and 6 mg kg<sup>-1</sup> (MAR16-02: 5.87 ± 0.26 mg kg<sup>-1</sup>; DAM17-02: 4.00 ± 0.33 mg kg<sup>-1</sup>).

283 The two sediment records showed high concentrations during the 1940s–1960s, following  
284 the trends determined for the Seine River (Lorgeoux et al., 2016). Notably, although the  
285 maximum levels measured by these authors were more than twice those measured for the  
286 lower reaches of the Eure River, the maximum values obtained in the Eure River were within  
287 the same order of magnitude as the concentrations measured in sediments collected  
288 downstream of the Marne River watershed (Ollivon et al., 2002). Moreover, the observed  
289 maxima were higher than those measured in other French watersheds, such as the Loire River  
290 watershed (Bertrand et al., 2015). Nonetheless, the Eure River watershed and the Eure River  
291 flow were ~13 and 30 times lower than those of the Seine River and ~20 and 50 times lower  
292 than those of the Loire River, showing the severity of PAH contamination in the Eure River  
293 watershed, particularly during the 1940s–1960s. Moreover, the obtained maxima were also  
294 higher than those measured in surface sediments of several large European lakes (Fernández  
295 et al., 1999), SPM from several large French and European rivers (Rhône, Tamar, Scheldt and  
296 Rhine rivers; Fernandes et al. (1999)), or in sediments from Canadian lakes located near an oil  
297 sands mining site (Ahad et al., 2015). Concentrations for the most recent deposits are  
298 comparable to those determined for recent sediment deposits in the Seine Basin (Lorgeoux et  
299 al., 2016), SPM collected in the Seine River (Gasperi et al., 2009), or concentrations

300 measured in the Loire River watershed since the late 1980s (Bertrand et al., 2015). In  
301 addition, some PAH concentrations recorded during the 1940s–1960s exceeded the probable  
302 effect concentrations (PECs; equal to  $22.8 \text{ mg kg}^{-1}$  for total PAHs) defined by MacDonald et  
303 al. (2000), as the level above which effects on benthic biota are likely to be observed,  
304 demonstrating the potential toxicity of the accumulated sediments, especially in case of  
305 remobilization.

306 The reconstruction of PAH temporal trends therefore demonstrated significant PAH  
307 contamination but did not provide information on the sources responsible for these  
308 contaminations. To achieve this, it was necessary to study the distribution of isomers over  
309 time (Yunker et al., 2002).

310

### 311 *3.3.2. Distribution of PAH molar weights and isomers throughout the cores*

312 The abundances of 2-ring PAHs (mass 128; Na) were <1% and those of 3-ring PAHs  
313 (masses 152, 154, 166, and 178) were between 11–23% and 10–18% of the total PAHs for  
314 MAR16-02 and DAM17-02, respectively. Pn and An (mass 178) were the main components  
315 of this fraction, representing on average between 11.1% and 12.4% of the total PAHs. 4-ring  
316 PAHs (masses 202 and 228) were mostly represented with abundances between 34–51%  
317 (MAR16-02) and 36–46% (DAM17-02). The abundances of the 5-ring PAHs (masses 252  
318 and 278) were between 24–42% (MAR16-02) and 25–30% (DAM17-02). The abundances of  
319 6-ring PAHs (mass 276; IP and Bghi isomers) were between 7–15% (MAR16-02) and 11–  
320 25% (DAM17-02).

321 This important contribution of 4-, 5-, and 6-ring PAHs has been observed in other French  
322 watersheds (e.g. Seine River watershed (Lorgeoux et al., 2016); Loire River watershed  
323 (Bertrand et al., 2015)) and is frequently observed in sediments downstream or adjacent to  
324 industrialized and/or urbanized areas (Yunker et al., 2002). Isomers with masses of 202, 228,



325 252, and 276 are the major components of gasoline and diesel soot, as well as coal  
326 combustion emissions, of which the 202- and 252-mass isomers are predominant (Wang et al.,  
327 1999; Yunker et al., 2002). Low molecular weight (LMW) PAHs (2-3-rings) are more  
328 abundant in petrogenic products and low- to moderate-temperature combustion processes (e.g.  
329 biomass and coal burning in homes), whereas high molecular weight (HMW) PAHs (5-6-  
330 rings) are products of high-temperature combustion of coal or petroleum from large power  
331 plants and factories or vehicular emissions (Ding et al., 2014). Thus, sediments of the lower  
332 reaches of the Eure River exhibited an anthropogenic pyrogenic PAH signature (Yunker et al.,  
333 2002), which can partly explain the strong correlation between PAHs and refractory  $C_{org}$  in  
334 the sediments. Indeed, soot is mainly composed of refractory  $C_{org}$  (Poot et al., 2014) and the  
335 strong link between PAHs and RC/TOC could confirm a predominant atmospheric input of  
336 PAHs (especially heavy PAHs) through soot from combustion processes. Nevertheless, this  
337 hypothesis must be further confirmed, as the link between PAHs and refractory  $C_{org}$  could  
338 occur during transport or deposition of the latter on the watershed soils.

339 In addition to discriminating between pyrogenic and petrogenic sources, diagnostic PAH  
340 ratios can be used to distinguish combustion sources (e.g. petroleum, coal, or wood  
341 combustion) (Yunker et al., 2002). Therefore, different diagnostic ratios based on the ratios of  
342 light and heavy PAHs were calculated (Fig. 5). The Fl and Py isomers were the first and third  
343 most abundant isomers for MAR16-02 (Fl: 14.5%; Py: 12.1%) and DAM17-02 (Fl: 16.6%;  
344 Py: 13.6%), respectively. All Fl/(Fl+Py) ratios exceeded 0.5 ( $Fl/(Fl+Py)_{mean} = 0.54 \pm 0.01$  for  
345 MAR16-02 and  $Fl/(Fl+Py)_{mean} = 0.55 \pm 0.01$  for DAM17-02), which is suggestive of a strong  
346 preponderance of coal and/or wood combustion as the main sources of PAH contamination  
347 (Budzinski et al., 1997; Yunker et al., 2002), as in the Seine River watershed (Lorgeoux et al.,  
348 2016). Moreover, the BaA and Ch isomers were among the most abundant for MAR16-02  
349 (BaA: 8.8%; Ch: 8.4%) and DAM17-02 (BaA: 6.4%; Ch: 6.5%). The calculated BaA/228

350 (BaA / (BaA + Ch) vs Fl/(Fl+Py)) ratios were all greater than 0.45 (BaA/228<sub>mean</sub> = 0.51 ± 0.02  
351 for MAR16-02; BaA/228<sub>mean</sub> = 0.50 ± 0.05 for DAM17-02), which also suggests that the  
352 PAHs stored in the ponds of the lower reaches of the Eure River had pyrogenic rather than  
353 petrogenic source signatures (Fig. 5A) (Yunker et al., 2002). However, no logic was  
354 established in terms of temporality because the set of calculated ratios was limited to a  
355 restricted domain with little variability.

356 The average ratios obtained from the isomers of mass 276 (IP/(IP+Bghi) vs Fl/(Fl+Py)) were  
357 greater than 0.5 (IP/(IP+Bghi)<sub>mean</sub> = 0.53 ± 0.02 for MAR16-02; IP/(IP+Bghi)<sub>mean</sub> = 0.53 ±  
358 0.04 for DAM17-02) but some values were below 0.5 (Fig. 5B). Fig. 5B shows that a  
359 temporal trend could be identified: the IP/(IP+Bghi) ratio was below 0.5 the mid-1980s for  
360 MAR16-02 and DAM17-02, due to an increase in the contribution of isomers with a mass of  
361 276. This indicates that sources linked to petroleum combustion intensified from the late  
362 1980s onwards; however, the BaA/228 ratio (Fig. 5A) was not descriptive of this temporal  
363 evolution. BaA (MW = 228) and BaP (MW = 278) have been shown to be more sensitive to  
364 photodegradation than most other PAHs (except An) when emitted to the atmosphere (Yunker  
365 et al., 2002). Therefore, given that isomers with masses of 276 and 202 are more stable than  
366 those with masses of 278 and 228, their use in diagnostic ratios allows for a better  
367 differentiation between combustion sources without significant artefacts related to their  
368 subsequent transformations.

369 The An/178 (An/(An+Pn) vs Fl/(Fl+Py)) ratios obtained for the two sediment records were  
370 greater than 0.1 (Fig. 5C). A ratio of 0.1 indicates a very small proportion of An relative to  
371 Pn. This is likely associated with substantial An photodegradation (i.e. given that An is much  
372 less stable than Pn) from the combustion source to its final deposition via atmospheric  
373 transport. On the other hand, the greater the distance from the combustion source to the  
374 deposition zone, the more the ratio tends towards 0.1 (Yunker et al., 2002). However, in

375 contrast to previously studied ratios, the An/178 ratio averages are significantly different  
376 within the two sediment records ( $An/178_{\text{mean}} = 0.41 \pm 0.09$  for MAR16-02;  $An/178_{\text{mean}} = 0.25$   
377  $\pm 0.04$  for DAM17-02) and their temporal trends were also distinct. In the case of the  
378 DAM17-02 core, the ratio generally tended towards 0.10 from the 1940s to the present day,  
379 i.e. towards a source corresponding mainly to combustion. This was also true for the MAR16-  
380 02 core after the 1990s. However, the An/178 ratio for the MAR16-02 core exhibited high  
381 values ( $> 0.4$ ) over the mid-1960s–1990s due to an increase in An concentrations throughout  
382 this period. Within the Seine River watershed, an enrichment in An in sediments was also  
383 recorded from 1971 onwards, without its origin being determined (Lorgeoux et al., 2016). It  
384 would appear that for the sediments of the Martot Pond, this increase started a few years  
385 earlier and stopped around the 1990s. Nonetheless, these inputs may share the same origin,  
386 which could be attributed to oil discharges in an aquatic system that did not undergo  
387 combustion. As the transport of PAHs was not carried out through the atmosphere, An was  
388 not affected by photodegradation and its concentration thus remained close to that of Pn  
389 (Tobiszewski and Namieśnik, 2012). As mentioned previously, Martot Pond was likely  
390 impacted by the contributions of the Seine estuary during tidal flows, which is not the case for  
391 Les Damps Pond, located upstream. However, Martot Pond is close to the industrial areas of  
392 Rouen, which were marked by strong petrochemical activity and significant river transport of  
393 oil between the 1960s and 1990s. It appears that after the 1990s, oil leaks during transport  
394 greatly decreased, leaving combustion processes as the only sources of sediment  
395 contamination.

396

### 397 3.4. PCBs in sediments cores

398

#### 399 3.4.1. General PCB trends in sediment cores

400 Total PCB concentrations were recorded for the MAR16-02 and DAM17-02 cores (Fig. 6).  
401 PCBs were not detected in the Seine Unit (78–90 cm) of MAR16-02 core. In contrast, the  
402 Eure Unit of MAR16-02 and DAM17-02 exhibited concentrations ranging between 0.02–1.57  
403  $\text{mg kg}^{-1}$  ( $\text{PCB}_{\text{mean}} = 0.72 \pm 0.05 \text{ mg kg}^{-1}$ ) and 0.09–1.60  $\text{mg kg}^{-1}$  ( $\text{PCB}_{\text{mean}} = 0.50 \pm 0.06 \text{ mg}$   
404  $\text{kg}^{-1}$ ). For MAR16-02, PCBs levels increased at the transition between the two sedimentary  
405 facies and reached a peak of  $1.57 \pm 0.06 \text{ mg kg}^{-1}$  in the late 1950s, whereas a  $1.60 \pm 0.12 \text{ mg}$   
406  $\text{kg}^{-1}$  peak was recorded in DAM17-02 in the late 1960s. A general downward trend in PCB  
407 levels was then visible up to the surface of the sediment deposits. For MAR16-02, two  
408 concentration peaks were observed despite the downward trend, the first around 1976 ( $\text{PCB} =$   
409  $0.68 \pm 0.13 \text{ mg kg}^{-1}$ ) and the second in 1992–1996 with an extremely high concentration that  
410 reached  $16.8 \text{ mg kg}^{-1}$ . For the most recent sediment deposits (from the 2000s onward),  
411 concentrations are relatively close or equal to  $0.12 \pm 0.01 \text{ mg kg}^{-1}$  and  $0.18 \pm 0.05 \text{ mg kg}^{-1}$  for  
412 MAR16-02 and DAM17-02, respectively.

413 The general temporal trend of PCB contents was similar to previously reported trends in  
414 France (Seine River watershed: Lorgeoux et al., 2016; Rhône River watershed: Desmet et al.,  
415 2012), Europe (UK: Sanders et al., 1992; Germany: Bruckmeier et al., 1997; Italy: Combi et  
416 al., 2020), and the US (Christensen and Lo, 1986; Van Metre et al., 1997), and were similar to  
417 temporal trends in global PCB production and consumption (Breivik et al., 2002). The  
418 maxima obtained during the 1950s–1970s ( $\sim 1.6 \text{ mg kg}^{-1}$  for the two ponds) were higher than  
419 those historically recorded in several French watersheds, such as the Loire ( $1.2 \text{ mg kg}^{-1}$ ,  
420 Dendievel et al., 2019), Garonne ( $0.145 \text{ mg kg}^{-1}$ , Dendievel et al., 2019) and Rhône rivers  
421 watersheds ( $0.28 \text{ mg kg}^{-1}$ , Desmet et al., 2012;  $0.42 \text{ mg kg}^{-1}$ , Mourier et al., 2014); European  
422 watersheds such as the Brno Reservoir, Czech Republic ( $0.08 \text{ mg kg}^{-1}$ , Franců et al., 2010);  
423 the Esthwaite Water, England ( $0.05 \text{ mg kg}^{-1}$ , Sanders et al., 1992); or the Chattahoochee River  
424 watershed, US ( $0.38 \text{ mg kg}^{-1}$ , Van Metre et al., 1997). It should be noted that total PCB

425 concentrations were calculated from 7 congeners in the cited studies and up to 22 for Sanders  
426 et al. (1992), compared with the 6 congeners studied herein. Nevertheless, the maximum  
427 concentrations recorded in the Eure River watershed remain lower than those recorded in  
428 recent flood deposits in the Rhône River (Dendievel et al., 2019), the Seine River (2.31 mg  
429 kg<sup>-1</sup>, Lorgeoux et al., 2016), or the Seine estuary, France (5 mg kg<sup>-1</sup>; Dendievel et al., 2019),  
430 the Lippe River, Germany (2.63 mg kg<sup>-1</sup>, Heim et al., 2004), or Milwaukee Harbour, US (13.4  
431 mg kg<sup>-1</sup>, Christensen and Lo, 1986).

432 The detection of PCBs prior to 1955 (i.e. the year in which PCB production and  
433 consumption in France began to increase; Lorgeoux et al., 2016) may be consistent with the  
434 fact that PCB production in France began approximately in the 1930s (de Voogt and  
435 Brinkman, 1989). However, the maximum consumption recorded in France in 1975 does not  
436 correspond to the maximum concentrations in sediments recorded a few years earlier. The  
437 year 1975 also corresponds to the first bans on the use of PCBs in open systems (e.g.  
438 plasticizers, carbonless copy paper, lubricants, inks, laminating and impregnating agents,  
439 paints, adhesives, waxes, cement and plaster additives, casting and dedusting agents, sealing  
440 liquids, fire retardants, immersion oils, and pesticides (de Voogt and Brinkman, 1989; Bigus  
441 et al., 2014)), which may explain why it was after this date that the levels started to show a  
442 substantial decrease, especially in Martot Pond. Additionally, PCB concentrations began to  
443 stabilise to low levels in the early 1990s (with the exception of the 1992–1996 period in  
444 Martot Pond), which can be linked to the cessation of PCB production in France in 1984 (de  
445 Voogt and Brinkman, 1989) coupled with the ban on PCB use in France in 1987, including in  
446 closed-system applications (e.g. cooling liquids in transformers, dielectric liquids in large and  
447 small capacitors, heat-conducting fluids in heat-exchangers and fire- or heat-resistant  
448 corrosion-free hydraulic fluids in mining equipment and vacuum pumps (de Voogt and  
449 Brinkman, 1989; Kannan et al., 1992; Bigus et al., 2014)). In addition, some PCB

450 concentrations recorded during the 1950s–1960s exceeded the probable effect concentrations  
451 (PECs; equal to 0.676 mg kg<sup>-1</sup> for total PCBs) defined by MacDonald et al. (2000), as the  
452 level above which effects on benthic biota are likely to be observed, demonstrating the  
453 potential toxicity of the accumulated sediments, especially in case of remobilization.

454 Thus, the temporal reconstruction of PCB levels demonstrated a significant PCB  
455 contamination within the Eure River watershed, but only an analysis of the distribution of the  
456 congeners can allow for the determination of the contaminant sources.

457

#### 458 3.4.2. *Distribution of PCB congeners*

459 Congener distributions were recorded for the MAR16-02 and DAM17-02 cores (Fig. 6). For  
460 the Eure Unit of MAR16-02 core, PCB180 was, on average, predominantly represented  
461 (23.1%), followed by PCB138 (22.1%), PCB153 (20.2%), PCB101 (15.0%), PCB52 (11.3%),  
462 and PCB28 (8.2%). Therefore, 6-chlorine PCBs (PCB138 + PCB153) were predominantly  
463 represented (42.3%). For DAM17-02, PCB138 represented on average 42.8% of the  $\sum$ PCBs,  
464 which combined with PCB153 (8.1%) amounted to a 50.9% representation of 6-Chlorine  
465 PCBs, whereas PCB101 represented on average 20.7%, followed by PCB180 (18.8%),  
466 PCB52 (5.9%), and PCB28 (3.7%). PCB28, the globally least represented congener, was  
467 detected beginning in the early 1950s, and its contribution has generally followed the trends  
468 shown by PCB concentrations. However, during the peak of PCB levels in the late 1950s for  
469 MAR16-02 and the 1960s for DAM17-02, PCB28 was the most represented congener (25.4%  
470 and 26.5% respectively). From the late 1970s onwards, PCB28 represented less than 10% of  
471  $\sum$ PCBs for MAR16-02, whereas it was almost no longer detected in DAM17-02. PCB52, the  
472 second least represented congener, was detected from the beginning of the sediment records  
473 and, similar to PCB28, followed the overall global PCB trends. However, PCB52 was the  
474 second most represented congener during the 1950s peak concentration (21.7%) for MAR16-

475 02 and the third (21.9%) during the 1960s peak for DAM17-02. The contribution of this  
476 isomer decreased overall afterwards (< 10%). PCB101 and PCB153 followed similar trends  
477 for MAR16-02, with a strong representation at the Eure/Seine unit transition (>30%) and then  
478 decreased as the PCB concentration increased. Following the peak PCB concentration, the  
479 contribution of PCB101 decreased, although its contribution was approximately 20%,  
480 whereas the contribution of PCB153 also stabilised at approximately 20%. PCB138 also  
481 showed strong contributions from the Eure/Seine unit transition of the MAR16-02 core, which  
482 also decreased as the PCB concentration increased. Afterwards, the contribution of PCB138  
483 increased overall towards the surface as the PCB concentrations decreased. The distribution of  
484 PCB101 was also important at the beginning of the DAM17-02 core (>40%). For the  
485 MAR16-02 core, this congener decreased as PCB concentrations increased. In contrast to  
486 MAR16-02, the contribution of PCB153 was low for DAM17-02 and showed an increasing  
487 trend until the early 1980s (~17%). The contribution of PCB138 showed a broadly similar  
488 behaviour to that of PCB153 and reached nearly 70% at the end of the 1980s. Finally,  
489 PCB180 was only detected from the mid-1950s for MAR16-02 but its contribution increased  
490 over time and was very significant from the late 1990s onwards. Conversely, PCB180 showed  
491 a strong contribution at the beginning of the DAM17-02 record, which decreased with  
492 increasing PCB concentration.

493 Releases of PCBs to the environment can result from inputs to watercourses through leakage  
494 from facilities or discharges from landfills, as well as leaching from industrial or urban  
495 surfaces, but also from atmospheric deposition, in which case PCBs are mostly transported in  
496 particulate form (Zhou et al., 2001; Yang et al., 2012). More generally, industrial activities  
497 and urbanization are the primary causes of sediment PCB pollution (Bigus et al., 2014).  
498 France was one of the first countries to produce PCBs and is estimated to have contributed  
499 approximately 10% of the global production from 1930 to 1984 (i.e. 134,654 t of the 1.5 Mt

500 produced globally) (de Voogt and Brinkman, 1989; Breivik et al., 2002). PCBs in France  
501 were produced under the names "Phenoclor" and "Pyrалene". Moreover, it can be assumed  
502 that the "PCB technical mixture" used in France prior to 1987 was predominantly produced in  
503 France, regardless of its form and use.

504 Comparing PCB isomers (and thus comparing PCBs according to their chlorination degree)  
505 can be useful to identify the sources responsible for PCB releases to the environment and to  
506 assess changes in their use within a given watershed (Franců et al., 2010; Cai et al., 2016).  
507 Ratios of PCB<sub>28</sub>/PCB<sub>153</sub> and PCB<sub>(28+53)</sub>/PCB<sub>(138+153+180)</sub> congeners were found to be  
508 below 1 for most of the MAR16-02 (mean = 0.43 and 0.36, respectively) and DAM17-02  
509 (mean = 0.61 and 0.17, respectively) cores (Fig. 7), confirming a dominance of "high  
510 chlorinated congeners" that are generally present in the composition of hydraulic fluids or  
511 thermostable lubricants, whereas "lower chlorinated mixtures" are used for less viscous  
512 applications (Franců et al., 2010). However, these ratios were greater than 1 during the high-  
513 concentration instances recorded in the late 1950s (Martot Pond) and 1960s (Les Damps  
514 Pond), confirming the dominance of "low chlorinated congeners" during these periods (Fig.  
515 7). This could be explained by a contribution from at least two distinct sources during certain  
516 periods of high PCB use. If the production and use of formulations containing highly  
517 chlorinated PCBs were staggered over the period spanning from the 1930s to the late 1980s,  
518 the temporary dominance of low chlorinated congeners (tri-Cl and tetra-Cl) may indicate the  
519 use and subsequent release of specific technical PCB mixtures, such as DP-3 or DP-4 (i.e. two  
520 types of Phenoclor mixtures). These technical mixtures are equivalent to the Aroclor 1016 and  
521 1242 mixtures (Kannan et al., 1992; Breivik et al., 2002), which are mainly composed PCBs  
522 containing 2–5 chlorines (Frame, 1997; Breivik et al., 2002). These observations are  
523 consistent with the reports of Franců et al. (2010) (Brno Reservoir, Czech Republic), whereby  
524 the temporary dominance of lower chlorinated congeners corresponded to (accidental) input



525 from a former transformer and capacitor manufacturing plant that used a low chlorinated  
526 technical PCB mixture called Delor 103 (equivalent to Aroclor 1242, which is produced in the  
527 US). As previously reported by Cai et al. (2016) and Yang et al. (2012), the predominance of  
528 heavy congeners could correspond to atmospheric inputs over long distances. However, this  
529 occurred in countries that were not direct producers of PCBs at the time of deposition. Other  
530 authors indicate that the presence of lighter PCBs is more suggestive of substantial  
531 atmospheric contribution, given that these congeners are more susceptible to long-range  
532 transport as they are less prone to photodegradation than highly chlorinated PCBs. Therefore,  
533 the predominance of heavier PCBs seems to suggest a larger contribution of emissions from  
534 local sources (Alegria et al., 2016). Halfadji et al. (2019) noted that sites contaminated with  
535 highly chlorinated PCBs were near petrochemical industrial zones, which is also the case for  
536 Martot Pond.

537 It should be noted that during the pollution peak recorded in Martot Pond during the 1992–  
538 1996 period, the previously calculated ratios remained below 1, demonstrating the occurrence  
539 of a pollution source that was distinct from that responsible for the heavy contamination a few  
540 decades earlier. Given that the studied area was not impacted by major leaks associated with  
541 the degradation of electrical installations, this sudden increase in contamination level could be  
542 attributed to a very localised wild discharge. Notably, Les Damps Pond (located upstream) did  
543 not show this intense pollution peak and the pollution date occurred very shortly after the ban  
544 on the use of PCBs in France. Unfortunately, some industrial discharges continued even after  
545 1987, as was the case in the Rhone River watershed, where high PCB concentrations were  
546 recorded several years after cessation of their use (Desmet et al., 2012).

547

#### 548 **4. Conclusions**

549

550 This study demonstrated that PAHs, particularly heavy PAHs, had a high affinity for  
551 refractory  $C_{org}$ , whereas PCBs showed a lower affinity. The Eure River watershed has been  
552 subject to significant POP contaminations since the 1940s, corresponding to the same order of  
553 magnitude as that recorded in other French or European watersheds. The abundance of  
554 different PAH isomers and their diagnostic ratios demonstrated that the high concentrations of  
555 PAHs recorded during the 1940s–1960s were of pyrogenic origin (i.e. derived from  
556 combustion processes), whereas certain signatures recorded in more recent deposits (up to the  
557 1990s) exhibited an evolution towards a petrogenic origin. Furthermore, PCB temporal trends,  
558 particularly their high concentrations during the 1950s–1970s, are generally linked to the  
559 production, consumption, and bans on the use of PCBs in France. The distribution of PCB  
560 congeners and certain congener ratios demonstrated that the high releases during the 1950s–  
561 1970s were likely linked to the release of "technical mixtures PCBs" composed of "low  
562 chlorinated congeners" into the river, whereas the most recent inputs were mainly attributed to  
563 atmospheric inputs of "high chlorinated congeners", with the exception of a local high  
564 undefined contamination recorded in Martot Pond.

565

## 566 **Acknowledgements**

567 This work is part of the OSS 276 project, financially supported by the Seine-Normandie  
568 Water Agency (France). This work is support by the CNRS toward EC2CO grant (Avant-  
569 Seine project). Gardes Th. grant was funded by the Region Normandie, which supports the  
570 scientific consortium SCALE UMR CNRS 3730. CNRS also supports the French national  
571 cyber-Repository (<https://www.cybercarotheque.fr/>) which is a portal for metadata associated  
572 with marine, lake/river sediment cores stored in French laboratories. This project was initiated  
573 by CLIMCOR project (<http://climcor-equipex.dt.insu.cnrs.fr/>).

574 Our paper is a contribution to ROZA-LTER-fr project : Retro-Observatory of sedimentary  
575 Archive from French LTER (<http://ccwbvps18.in2p3.fr/maps/visualiseur-coyoxhup#project>)  
576 which is a portal for data associated with marine, lake sediment cores stored in LTER French  
577 laboratories.

578

579 **References**

580

- 581 Ab Razak, I.A., Li, A., Christensen, E.R., 1996. Association of PAHs, PCBs, 137Cs, and 210Pb with  
582 clay, silt, and organic carbon in sediments. *Water Science and Technology, Water Quality*  
583 *International '96 Part 4* 34, 29–35. [https://doi.org/10.1016/S0273-1223\(96\)00719-6](https://doi.org/10.1016/S0273-1223(96)00719-6)
- 584 Abarnou, A., Avoine, J., Dupont, J.P., Lafite, R., Simon, S., 1987. Role of suspended sediments on the  
585 distribution of PCB in the Seine Estuary (France). *Continental Shelf Research, Dynamics of*  
586 *Turbid Coastal Environments* 7, 1345–1350. [https://doi.org/10.1016/0278-4343\(87\)90038-0](https://doi.org/10.1016/0278-4343(87)90038-0)
- 587 Ahad, J.M.E., Jautzy, J.J., Cumming, B.F., Das, B., Laird, K.R., Sanei, H., 2015. Sources of  
588 polycyclic aromatic hydrocarbons (PAHs) to northwestern Saskatchewan lakes east of the  
589 Athabasca oil sands. *Organic Geochemistry* 80, 35–45.  
590 <https://doi.org/10.1016/j.orggeochem.2015.01.001>
- 591 Alegria, H., Martinez-Colon, M., Birgul, A., Brooks, G., Hanson, L., Kurt-Karakus, P., 2016.  
592 Historical sediment record and levels of PCBs in sediments and mangroves of Jobos Bay,  
593 Puerto Rico. *Science of The Total Environment* 573, 1003–1009.  
594 <https://doi.org/10.1016/j.scitotenv.2016.08.165>
- 595 Bertrand, O., Mondamert, L., Grosbois, C., Dhivert, E., Bourrain, X., Labanowski, J., Desmet, M.,  
596 2015. Storage and source of polycyclic aromatic hydrocarbons in sediments downstream of a  
597 major coal district in France. *Environmental Pollution* 207, 329–340.  
598 <https://doi.org/10.1016/j.envpol.2015.09.028>
- 599 Bigus, P., Tobiszewski, M., Namieśnik, J., 2014. Historical records of organic pollutants in sediment  
600 cores. *Marine Pollution Bulletin* 78, 26–42. <https://doi.org/10.1016/j.marpolbul.2013.11.008>
- 601 Blanchard, M., Teil, M.-J., Guigon-Moreau, E., Larcher-Tiphagne, K., Ollivon, D., Garban, B.,  
602 Chevreuil, M., 2007. Persistent toxic substance inputs to the river Seine basin (France) via  
603 atmospheric deposition and urban sludge application. *The Science of the Total Environment*  
604 375.
- 605 Breivik, K., Sweetman, A., Pacyna, J.M., Jones, K.C., 2002. Towards a global historical emission  
606 inventory for selected PCB congeners — a mass balance approach: 1. Global production and  
607 consumption. *Science of The Total Environment* 290, 181–198.  
608 [https://doi.org/10.1016/S0048-9697\(01\)01075-0](https://doi.org/10.1016/S0048-9697(01)01075-0)
- 609 Bruckmeier, B.F.A., Jüttner, I., Schramm, K.-W., Winkler, R., Steinberg, C.E.W., Kettrup, A., 1997.  
610 PCBs and PCDD/Fs in lake sediments of Großer Arbersee, Bavarian Forest, South Germany.  
611 *Environmental Pollution* 95, 19–25. [https://doi.org/10.1016/S0269-7491\(96\)00118-2](https://doi.org/10.1016/S0269-7491(96)00118-2)
- 612 Budzinski, H., Jones, I., Bellocq, J., Piérard, C., Garrigues, P., 1997. Evaluation of sediment  
613 contamination by polycyclic aromatic hydrocarbons in the Gironde estuary. *Marine*  
614 *Chemistry, 4th International Symposium on the Biogeochemistry of Model Estuaries* 58, 85–  
615 97. [https://doi.org/10.1016/S0304-4203\(97\)00028-5](https://doi.org/10.1016/S0304-4203(97)00028-5)
- 616 Burgess, R.M., Ryba, S.A., Cantwell, M.G., Gundersen, J.L., 2001. Exploratory Analysis of the  
617 Effects of Particulate Characteristics on the Variation in Partitioning of Nonpolar Organic  
618 Contaminants to Marine Sediments. *Water Research* 35, 4390–4404.  
619 [https://doi.org/10.1016/S0043-1354\(01\)00179-8](https://doi.org/10.1016/S0043-1354(01)00179-8)

- 620 Cai, Y., Wang, X., Wu, Y., Li, Y., Ya, M., 2016. Over 100-year sedimentary record of polycyclic  
621 aromatic hydrocarbons (PAHs) and organochlorine compounds (OCs) in the continental shelf  
622 of the East China Sea. *Environmental Pollution* 219, 774–784.  
623 <https://doi.org/10.1016/j.envpol.2016.07.053>
- 624 Callender, E., 2000. Geochemical effects of rapid sedimentation in aquatic systems: minimal  
625 diagenesis and the preservation of historical metal signatures. *Journal of Paleolimnology* 23,  
626 243–260. <https://doi.org/10.1023/A:1008114630756>
- 627 Carrie, J., Sanei, H., Stern, G., 2012. Standardisation of Rock–Eval pyrolysis for the analysis of recent  
628 sediments and soils. *Organic Geochemistry* 46, 38–53.  
629 <https://doi.org/10.1016/j.orggeochem.2012.01.011>
- 630 Chevreuil, M., Blanchard, M., Teil, M.J., Chesterikoff, A., 1998. Polychlorobiphenyl behaviour in the  
631 water/sediment system of the Seine river, France. *Water Research* 32, 1204–1212.  
632 [https://doi.org/10.1016/S0043-1354\(97\)00328-X](https://doi.org/10.1016/S0043-1354(97)00328-X)
- 633 Chevreuil, M., Chesterikoff, A., Létolle, R., Granier, L., 1989. Atmospheric pollution and fallout by  
634 PCBs and organochlorine pesticides (Ile-De-France). *Water Air Soil Pollut* 43, 73–83.  
635 <https://doi.org/10.1007/BF00175584>
- 636 Chevreuil, M., Granier, L., 1991. Seasonal cycle of polychlorinated biphenyls in the waters of the  
637 catchment basin of the river seine (France). *Water Air Soil Pollut* 59, 217–229.  
638 <https://doi.org/10.1007/BF00211831>
- 639 Chevreuil, M., Granier, L., Chesterikoff, A., Létolle, R., 1990. Polychlorinated biphenyls partitioning  
640 in waters from river, filtration plant and wastewater plant: the case for paris (france). *Water*  
641 *Research* 24, 1325–1333. [https://doi.org/10.1016/0043-1354\(90\)90149-Z](https://doi.org/10.1016/0043-1354(90)90149-Z)
- 642 Christensen, E.R., Lo, C.-K., 1986. Polychlorinated biphenyls in dated sediments of Milwaukee  
643 Harbour, Wisconsin, USA. *Environmental Pollution Series B, Chemical and Physical* 12, 217–  
644 232. [https://doi.org/10.1016/0143-148X\(86\)90011-X](https://doi.org/10.1016/0143-148X(86)90011-X)
- 645 Combi, T., Pintado-Herrera, M.G., Lara-Martín, P.A., Lopes-Rocha, M., Miserocchi, S., Langone, L.,  
646 Guerra, R., 2020. Historical sedimentary deposition and flux of PAHs, PCBs and DDTs in  
647 sediment cores from the western Adriatic Sea. *Chemosphere* 241, 125029.  
648 <https://doi.org/10.1016/j.chemosphere.2019.125029>
- 649 Copard, Y., Di Giovanni, C., Martaud, T., Albéric, P., Olivier, J.-E., 2006. Using Rock-Eval 6  
650 pyrolysis for tracking fossil organic carbon in modern environments: implications for the roles  
651 of erosion and weathering. *Earth Surface Processes and Landforms* 31, 135–153.  
652 <https://doi.org/10.1002/esp.1319>
- 653 de Voogt, P., Brinkman, U., 1989. Production, properties and usage of polychlorinated biphenyls, in:  
654 *Halogenated Biphenyls, Terphenyls, Naphtalenes, Dibenzodioxins and Related Products.*  
655 *Topics in Environmental Health.* pp. 3–45.
- 656 Décret n°87-59, 1987. Décret n°87-59 du 2 février 1987 relatif à la mise sur le marché, à l'utilisation  
657 et à l'élimination des polychlorobiphényles et polychloroterphényles, 87-59.
- 658 Dendievel, A.-M., Mourier, B., Coynel, A., Evrard, O., Labadie, P., Ayrault, S., Debret, M., Koltalo,  
659 F., Copard, Y., Faivre, Q., Gardes, T., Vauclin, S., Budzinski, H., Grosbois, C., Winiarski, T.,  
660 Desmet, M., 2019. Spatio-temporal assessment of the PCB sediment contamination in the four  
661 main French River Basins (1945–2018). *Earth System Science Data Discussions* 1–23.  
662 <https://doi.org/10.5194/essd-2019-167>
- 663 Desmet, M., Mourier, B., Mahler, B.J., Van Metre, P.C., Roux, G., Persat, H., Lefèvre, I., Peretti, A.,  
664 Chapron, E., Simonneau, A., Miège, C., Babut, M., 2012. Spatial and temporal trends in PCBs  
665 in sediment along the lower Rhône River, France. *Science of The Total Environment* 433,  
666 189–197. <https://doi.org/10.1016/j.scitotenv.2012.06.044>
- 667 Ding, S., Xu, Y., Wang, Y., Zhang, X., Zhao, L., Ruan, J., Wu, W., 2014. Spatial and Temporal  
668 Variability of Polycyclic Aromatic Hydrocarbons in Sediments from Yellow River-Dominated  
669 Margin [WWW Document]. *The Scientific World Journal.*  
670 <https://doi.org/10.1155/2014/654183>
- 671 Douglas, G.S., Bence, A.E., Prince, R.C., McMillen, S.J., Butler, E.L., 1996. Environmental Stability  
672 of Selected Petroleum Hydrocarbon Source and Weathering Ratios. *Environ. Sci. Technol.* 30,  
673 2332–2339. <https://doi.org/10.1021/es950751e>

- 674 Duursma, E.K., Nieuwenhuize, J., van Liere, J.M., 1989. Polychlorinated biphenyl equilibria in an  
675 estuarine system. *Science of The Total Environment* 79, 141–155.  
676 [https://doi.org/10.1016/0048-9697\(89\)90358-6](https://doi.org/10.1016/0048-9697(89)90358-6)
- 677 Fernandes, M.B., Sicre, M.-A., Boireau, A., Tronczynski, J., 1997. Polyaromatic hydrocarbon (PAH)  
678 distributions in the Seine River and its estuary. *Marine Pollution Bulletin* 34, 857–867.  
679 [https://doi.org/10.1016/S0025-326X\(97\)00063-5](https://doi.org/10.1016/S0025-326X(97)00063-5)
- 680 Fernandes, M.B., Sicre, M.-A., Broyelle, I., Lorre, A., Pont, D., 1999. Contamination by Polycyclic  
681 Aromatic Hydrocarbons (PAHs) in French and European rivers. *Hydrobiologia* 410, 343–348.  
682 <https://doi.org/10.1023/A:1003751629504>
- 683 Fernández, P., Vilanova, R.M., Grimalt, J.O., 1999. Sediment Fluxes of Polycyclic Aromatic  
684 Hydrocarbons in European High Altitude Mountain Lakes. *Environ. Sci. Technol.* 33, 3716–  
685 3722. <https://doi.org/10.1021/es9904639>
- 686 Frame, G.M., 1997. A collaborative study of 209 PCB congeners and 6 Aroclors on 20 different  
687 HRGC columns1. Retention and coelution database. *Fresenius J Anal Chem* 357, 701–713.  
688 <https://doi.org/10.1007/s002160050237>
- 689 Franců, E., Schwarzbauer, J., Lána, R., Nývlt, D., Nehyba, S., 2010. Historical Changes in Levels of  
690 Organic Pollutants in Sediment Cores from Brno Reservoir, Czech Republic. *Water Air Soil*  
691 *Pollut* 209, 81–91. <https://doi.org/10.1007/s11270-009-0182-x>
- 692 Gardes, T., Debret, M., Copard, Y., Coynel, A., Deloffre, J., Fournier, M., Revillon, S., Nizou, J.,  
693 Develle, A.-L., Sabatier, P., Marcotte, S., Patault, E., Faivre, Q., Portet-Koltalo, F., 2020a.  
694 Flux estimation, temporal trends and source determination of trace metal contamination in a  
695 major tributary of the Seine estuary, France. *Science of The Total Environment* 138249.  
696 <https://doi.org/10.1016/j.scitotenv.2020.138249>
- 697 Gardes, T., Debret, M., Copard, Y., Patault, E., Winiarski, T., Develle, A.-L., Sabatier, P., Dendievel,  
698 A.-M., Mourier, B., Marcotte, S., Leroy, B., Portet-Koltalo, F., 2020b. Reconstruction of  
699 anthropogenic activities in legacy sediments from the Eure River, a major tributary of the  
700 Seine Estuary (France). *CATENA* 190, 104513. <https://doi.org/10.1016/j.catena.2020.104513>
- 701 Gasperi, J., Garnaud, S., Rocher, V., Moilleron, R., 2009. Priority pollutants in surface waters and  
702 settleable particles within a densely urbanised area: Case study of Paris (France). *Science of*  
703 *The Total Environment* 407.
- 704 Granier, L.K., Chevreuril, M., 1997. Behaviour and spatial and temporal variations of polychlorinated  
705 biphenyls and lindane in the urban atmosphere of the Paris area, France. *Atmospheric*  
706 *Environment* 31, 3787–3802. [https://doi.org/10.1016/S1352-2310\(97\)00210-0](https://doi.org/10.1016/S1352-2310(97)00210-0)
- 707 Gschwend, P.M., Wu, Shianchee., 1985. On the constancy of sediment-water partition coefficients of  
708 hydrophobic organic pollutants. *Environ. Sci. Technol.* 19, 90–96.  
709 <https://doi.org/10.1021/es00131a011>
- 710 Halfadji, A., Touabet, A., Portet-Koltalo, F., Derf, F.L., Merlet-Machour, N., 2019. Concentrations  
711 and Source Identification of Polycyclic Aromatic Hydrocarbons (PAHs) and Polychlorinated  
712 Biphenyls (PCBs) in Agricultural, Urban/Residential, and Industrial Soils, East of Oran  
713 (Northwest Algeria). *Polycyclic Aromatic Compounds* 39, 299–310.  
714 <https://doi.org/10.1080/10406638.2017.1326947>
- 715 Hatzinger, P.B., Alexander, Martin., 1995. Effect of Aging of Chemicals in Soil on Their  
716 Biodegradability and Extractability. *Environ. Sci. Technol.* 29, 537–545.  
717 <https://doi.org/10.1021/es00002a033>
- 718 Heemken, O.P., Stachel, B., Theobald, N., Wenclawiak, B.W., 2000. Temporal Variability of Organic  
719 Micropollutants in Suspended Particulate Matter of the River Elbe at Hamburg and the River  
720 Mulde at Dessau, Germany. *Arch. Environ. Contam. Toxicol.* 38, 11–31.  
721 <https://doi.org/10.1007/s002449910003>
- 722 Heim, S., Schwarzbauer, J., Kronimus, A., Littke, R., Woda, C., Mangini, A., 2004. Geochronology of  
723 anthropogenic pollutants in riparian wetland sediments of the Lippe River (Germany). *Organic*  
724 *Geochemistry, Advances in Organic Geochemistry 2003. Proceedings of the 21st International*  
725 *Meeting on Organic Geochemistry* 35, 1409–1425.  
726 <https://doi.org/10.1016/j.orggeochem.2004.03.008>
- 727 Kannan, N., Schulz-bull, D.E., Petrick, G., Duinker, J.C., 1992. High Resolution PCB Analysis of  
728 Kanechlor, Phenoclor and Sovol Mixtures Using Multidimensional Gas Chromatography.

- 729 International Journal of Environmental Analytical Chemistry 47, 201–215.  
730 <https://doi.org/10.1080/03067319208027029>
- 731 Karickhoff, S.W., Brown, D.S., Scott, T.A., 1979. Sorption of hydrophobic pollutants on natural  
732 sediments. *Water Research* 13, 241–248. [https://doi.org/10.1016/0043-1354\(79\)90201-X](https://doi.org/10.1016/0043-1354(79)90201-X)
- 733 Lafargue, E., Marquis, F., Pillot, D., 1998. Rock-Eval 6 Applications in Hydrocarbon Exploration,  
734 Production, and Soil Contamination Studies. *Revue de l'Institut Français du Pétrole* 53, 421–  
735 437. <https://doi.org/10.2516/ogst:1998036>
- 736 Le Cloarec, M.-F., Bonte, P.H., Lestel, L., Lefèvre, I., Ayrault, S., 2011. Sedimentary record of metal  
737 contamination in the Seine River during the last century. *Physics and Chemistry of the Earth,*  
738 *Parts A/B/C, Man and River Systems: From pressures to physical, chemical and ecological*  
739 *status* 36, 515–529. <https://doi.org/10.1016/j.pce.2009.02.003>
- 740 Lorgeoux, C., Moilleron, R., Gasperi, J., Ayrault, S., Bonté, P., Lefèvre, I., Tassin, B., 2016. Temporal  
741 trends of persistent organic pollutants in dated sediment cores: Chemical fingerprinting of the  
742 anthropogenic impacts in the Seine River basin, Paris. *Science of The Total Environment* 541,  
743 1355–1363. <https://doi.org/10.1016/j.scitotenv.2015.09.147>
- 744 MacDonald, D.D., Ingersoll, C.G., Berger, T.A., 2000. Development and Evaluation of Consensus-  
745 Based Sediment Quality Guidelines for Freshwater Ecosystems. *Arch. Environ. Contam.*  
746 *Toxicol.* 39, 20–31. <https://doi.org/10.1007/s002440010075>
- 747 Marchand, M., 1989. Les PCB dans l'environnement marin. Aspects géochimiques d'apports et de  
748 distribution. *Cas du littoral français.* *rseau* 2, 373–403. <https://doi.org/10.7202/705036ar>
- 749 Means, J.C., Wood, S.G., Hassett, J.J., Banwart, W.L., 1980. Sorption of polynuclear aromatic  
750 hydrocarbons by sediments and soils. *Environ. Sci. Technol.* 14, 1524–1528.  
751 <https://doi.org/10.1021/es60172a005>
- 752 Meybeck, M., 2002. Riverine quality at the Anthropocene: Propositions for global space and time  
753 analysis, illustrated by the Seine River. *Aquat. Sci.* 64, 376–393.  
754 <https://doi.org/10.1007/PL00012593>
- 755 Mourier, B., Desmet, M., Van Metre, P.C., Mahler, B.J., Perrodin, Y., Roux, G., Bedell, J.-P., Lefèvre,  
756 I., Babut, M., 2014. Historical records, sources, and spatial trends of PCBs along the Rhône  
757 River (France). *Sci. Total Environ.* 476–477, 568–576.  
758 <https://doi.org/10.1016/j.scitotenv.2014.01.026>
- 759 Oliveira, César, Martins, N., Tavares, J., Pio, C., Cerqueira, M., Matos, M., Silva, H., Oliveira,  
760 Cristina, Camões, F., 2011. Size distribution of polycyclic aromatic hydrocarbons in a  
761 roadway tunnel in Lisbon, Portugal. *Chemosphere* 83, 1588–1596.  
762 <https://doi.org/10.1016/j.chemosphere.2011.01.011>
- 763 Ollivon, D., Garban, B., Blanchard, M., Teil, M.J., Carru, A.M., Chesterikoff, C., Chevreuil, M., 2002.  
764 Vertical Distribution and Fate of Trace Metals and Persistent Organic Pollutants in Sediments  
765 of the Seine and Marne Rivers (France). *Water, Air, & Soil Pollution* 134, 57–79.  
766 <https://doi.org/10.1023/A:1014194532128>
- 767 Page, D.S., Boehm, P.D., Douglas, G.S., Bence, A.E., Burns, W.A., Mankiewicz, P.J., 1999.  
768 Pyrogenic Polycyclic Aromatic Hydrocarbons in Sediments Record Past Human Activity: A  
769 Case Study in Prince William Sound, Alaska. *Marine Pollution Bulletin* 38, 247–260.  
770 [https://doi.org/10.1016/S0025-326X\(98\)00142-8](https://doi.org/10.1016/S0025-326X(98)00142-8)
- 771 Piérard, C., Budzinski, H., Garrigues, P., 1996. Grain-Size Distribution of Polychlorobiphenyls in  
772 Coastal Sediments. *Environ. Sci. Technol.* 30, 2776–2783. <https://doi.org/10.1021/es9600035>
- 773 Poot, A., Jonker, M.T.O., Gillissen, F., Koelmans, A.A., 2014. Explaining PAH desorption from  
774 sediments using Rock Eval analysis. *Environmental Pollution* 193, 247–253.  
775 <https://doi.org/10.1016/j.envpol.2014.06.041>
- 776 Quémerais, B., Lemieux, C., Lum, K.R., 1994. Concentrations and sources of PCBs and  
777 organochlorine pesticides in the St. Lawrence River (Canada) and its tributaries. *Chemosphere*  
778 29, 591–610. [https://doi.org/10.1016/0045-6535\(94\)90446-4](https://doi.org/10.1016/0045-6535(94)90446-4)
- 779 Salvadó, J.A., Grimalt, J.O., López, J.F., Durrieu de Madron, X., Pasqual, C., Canals, M., 2013.  
780 Distribution of organochlorine compounds in superficial sediments from the Gulf of Lion,  
781 northwestern Mediterranean Sea. *Progress in Oceanography, Integrated study of a deep*  
782 *submarine canyon and adjacent open slopes in the Western Mediterranean Sea: an essential*  
783 *habitat* 118, 235–248. <https://doi.org/10.1016/j.pocean.2013.07.014>

- 784 Sanders, G., Jones, K.C., Hamilton-Taylor, J., Doerr, H., 1992. Historical inputs of polychlorinated  
785 biphenyls and other organochlorines to a dated lacustrine sediment core in rural England.  
786 *Environ. Sci. Technol.* 26, 1815–1821. <https://doi.org/10.1021/es00033a016>
- 787 Shi, Z., Tao, S., Pan, B., Liu, W.X., Shen, W.R., 2007. Partitioning and source diagnostics of  
788 polycyclic aromatic hydrocarbons in rivers in Tianjin, China. *Environmental Pollution,*  
789 *Lichens in a Changing Pollution Environment* 146, 492–500.  
790 <https://doi.org/10.1016/j.envpol.2006.07.009>
- 791 Tobiszewski, M., Namieśnik, J., 2012. PAH diagnostic ratios for the identification of pollution  
792 emission sources. *Environmental Pollution* 162, 110–119.  
793 <https://doi.org/10.1016/j.envpol.2011.10.025>
- 794 Tsapakis, M., Stephanou, E.G., Karakassis, I., 2003. Evaluation of atmospheric transport as a nonpoint  
795 source of polycyclic aromatic hydrocarbons in marine sediments of the Eastern  
796 Mediterranean. *Marine Chemistry* 80, 283–298. [https://doi.org/10.1016/S0304-4203\(02\)00132-9](https://doi.org/10.1016/S0304-4203(02)00132-9)
- 798 US EPA, 2015. Toxic and Priority Pollutants Under the Clean Water Act [WWW Document]. URL  
799 <https://www.epa.gov/eg/toxic-and-priority-pollutants-under-clean-water-act> (accessed  
800 10.17.19).
- 801 Van Metre, P.C., Callender, E., Fuller, C.C., 1997. Historical Trends in Organochlorine Compounds in  
802 River Basins Identified Using Sediment Cores from Reservoirs. *Environ. Sci. Technol.* 31,  
803 2339–2344. <https://doi.org/10.1021/es960943p>
- 804 Van Metre, P.C., Mesnage, V., Laignel, B., Motelay, A., Deloffre, J., 2008. Origins of Sediment-  
805 Associated Contaminants to the Marais Vernier, the Seine Estuary, France. *Water Air Soil*  
806 *Pollut* 191, 331–344. <https://doi.org/10.1007/s11270-008-9628-9>
- 807 Wan, X., Pan, X., Wang, B., Zhao, S., Hu, P., Li, F., Boulanger, B., 2011. Distributions, historical  
808 trends, and source investigation of polychlorinated biphenyls in Dianchi Lake, China.  
809 *Chemosphere* 85, 361–367. <https://doi.org/10.1016/j.chemosphere.2011.06.098>
- 810 Wang, Z., Fingas, M., Shu, Y.Y., Sigouin, L., Landriault, M., Lambert, P., Turpin, R., Campagna, P.,  
811 Mullin, J., 1999. Quantitative Characterization of PAHs in Burn Residue and Soot Samples  
812 and Differentiation of Pyrogenic PAHs from Petrogenic PAHs—The 1994 Mobile Burn Study.  
813 *Environ. Sci. Technol.* 33, 3100–3109. <https://doi.org/10.1021/es990031y>
- 814 Yang, H., Zhuo, S., Xue, B., Zhang, C., Liu, W., 2012. Distribution, historical trends and inventories  
815 of polychlorinated biphenyls in sediments from Yangtze River Estuary and adjacent East  
816 China Sea. *Environmental Pollution, Interactions Between Indoor and Outdoor Air Pollution -*  
817 *Trends and Scientific Challenges* 169, 20–26. <https://doi.org/10.1016/j.envpol.2012.05.003>
- 818 Yunker, M.B., Macdonald, R.W., Vingarzan, R., Mitchell, R.H., Goyette, D., Sylvestre, S., 2002.  
819 PAHs in the Fraser River basin: a critical appraisal of PAH ratios as indicators of PAH source  
820 and composition. *Organic Geochemistry* 33, 489–515. [https://doi.org/10.1016/S0146-6380\(02\)00002-5](https://doi.org/10.1016/S0146-6380(02)00002-5)
- 822 Zennegg, M., Kohler, M., Hartmann, P.C., Sturm, M., Gujer, E., Schmid, P., Gerecke, A.C., Heeb,  
823 N.V., Kohler, H.-P.E., Giger, W., 2007. The historical record of PCB and PCDD/F deposition  
824 at Greifensee, a lake of the Swiss plateau, between 1848 and 1999. *Chemosphere,*  
825 *Halogenated Persistent Organic Pollutants Dioxin* 2004 67, 1754–1761.  
826 <https://doi.org/10.1016/j.chemosphere.2006.05.115>
- 827 Zhang, J., Cai, L., Yuan, D., Chen, M., 2004. Distribution and sources of polynuclear aromatic  
828 hydrocarbons in Mangrove surficial sediments of Deep Bay, China. *Marine Pollution Bulletin*  
829 49, 479–486. <https://doi.org/10.1016/j.marpolbul.2004.02.030>
- 830 Zhou, J.L., Maskaoui, K., Qiu, Y.W., Hong, H.S., Wang, Z.D., 2001. Polychlorinated biphenyl  
831 congeners and organochlorine insecticides in the water column and sediments of Daya Bay,  
832 China. *Environmental Pollution* 113, 373–384. [https://doi.org/10.1016/S0269-7491\(00\)00180-](https://doi.org/10.1016/S0269-7491(00)00180-9)  
833 9
- 834

**Table 1.** Sediment cores collected in Les Damps and Martot ponds (WGS 84).

Pond	Core ID	IGSN	Longitude (X)	Latitude (Y)	Core Length (cm)
LES	DAM15-02	IEM2C0016	1°10'9.05" E	49°18'16.13" N	80
DAMPS	DAM17-02	IEM2C000E	1°10'13.26" E	49°18'15.66" N	90
MARTOT	MAR15-01	IEM2C0001	1°03'1.68" E	49°17'49.68" N	138
	MAR16-02	IEM2C0008	1°03'2.60" E	49°17'49.30" N	129

**Table 2.** List of the analysed POPs.

PAHs			PCBs		
Compounds	Molar weight ( $g\ mol^{-1}$ )	X-Rings	Compounds	Molar weight ( $g\ mol^{-1}$ )	X-Chlorines
Naphthalene (Na)	128	2-Rings	PCB 28	258	3-Chlorine
Acenaphthylene (Ayl)	152	3-Rings	PCB 52	292	4-Chlorine
Acenaphthene (Aen)	154		PCB 101	326	5-Chlorine
Fluorene (F)	166		PCB 138	361	6-Chlorine
Phenanthrene (Pn)	178		PCB 153	361	6-Chlorine
Anthracene (An)			PCB 180	395	7-Chlorine
Fluoranthene (Fl)	202	4-Rings			
Pyrene (Py)					
Benz[ <i>a</i> ]anthracene (BaA)	228				
Chrysene (Ch)					
Benzo[ <i>b</i> ]fluoranthene (BbF)	252	5-Rings			
Benzo[ <i>k</i> ]fluoranthene (BkF)					
Benzo[ <i>a</i> ]pyrene (BaP)					
Dibenz[ <i>a,h</i> ]anthracene (DhA)	278				
Indeno[1,2,3- <i>cd</i> ]pyrene (IP)	276	6-Rings			
Benzo[ <i>ghi</i> ]perylene (Bghi)					



**Table 3.** Comparison of maximum PCB concentrations in sediment cores of several watersheds.

Location	Concentration (mg kg <sup>-1</sup> )	Time interval	References
<i>France</i>			
Eure River (lower section)	1.57 / 1.60	1950s–1970s	This study
Seine River (lower section)	2.31	1960	Lorgeoux et al., 2016
Seine estuary	5	1970s	Dendievel et al., 2019
Loire River (lower section)	1.2	1973–1989	
	1.4	2003–2008	
Garonne River (upper section)	0.145	1998	
Rhône River (lower section)	2.4 (flood deposits)	1995–1996	
	0.42	1990–1995	Mourier et al., 2014
	0.28	1991	Desmet et al., 2012
<i>Europe</i>			
Brno Reservoir (Czech Republic)	0.08	1970s–1980s	Franců et al., 2010
Lippe River (Germany)	2.63	1980–1985	Heim et al., 2004
Esthwaite Water (England)	0.05	1963	Sanders et al., 1992
<i>United States</i>			
Lake Harding (Chattahoochee River)	0.38	1950–1966	Van Metre et al., 1997
Milwaukee Harbour	13.4	1970–1975	Christensen and Lo, 1986

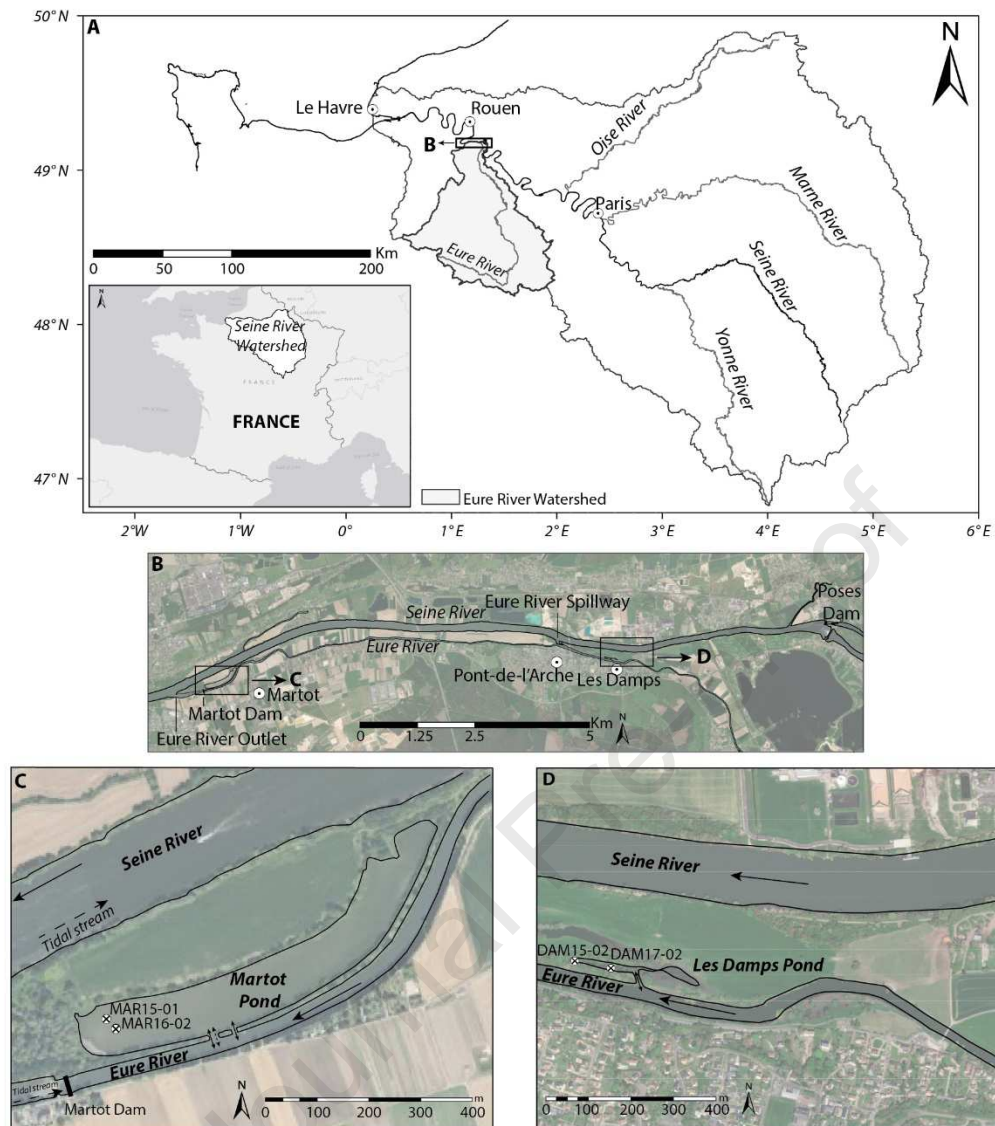


**Figure 1.** A. Seine River watershed; B. Study Area; C. Sediment core locations in Martot Pond and D. Sediment core locations in Les Damps Pond.

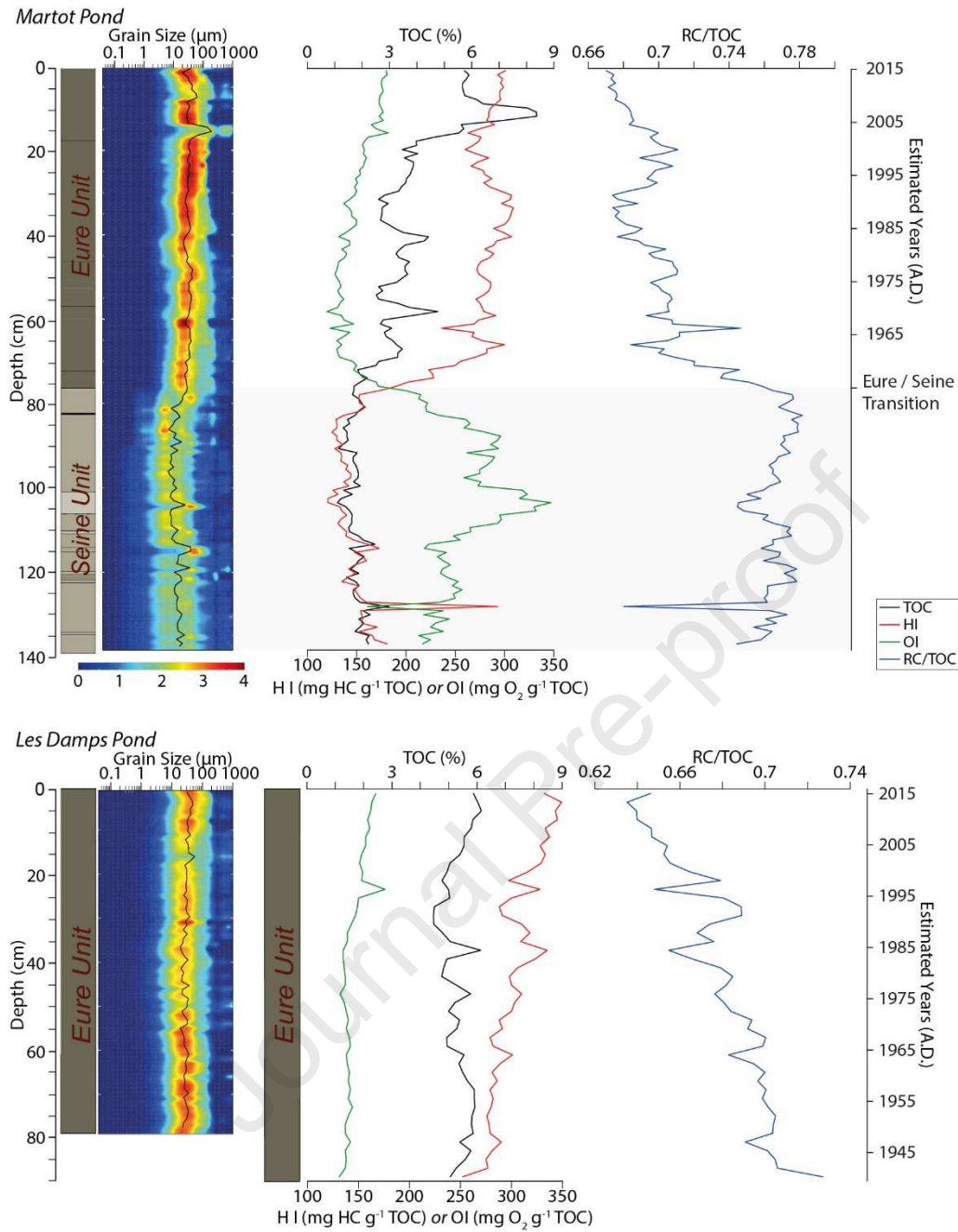


**Figure 2.** Grain size distribution,  $D_{50}$ , TOC, HI, OI, and RC/TOC for the MAR15-01 core (Martot Pond) and for the DAM15-02 and DAM17-02 cores (Les Damps Pond).

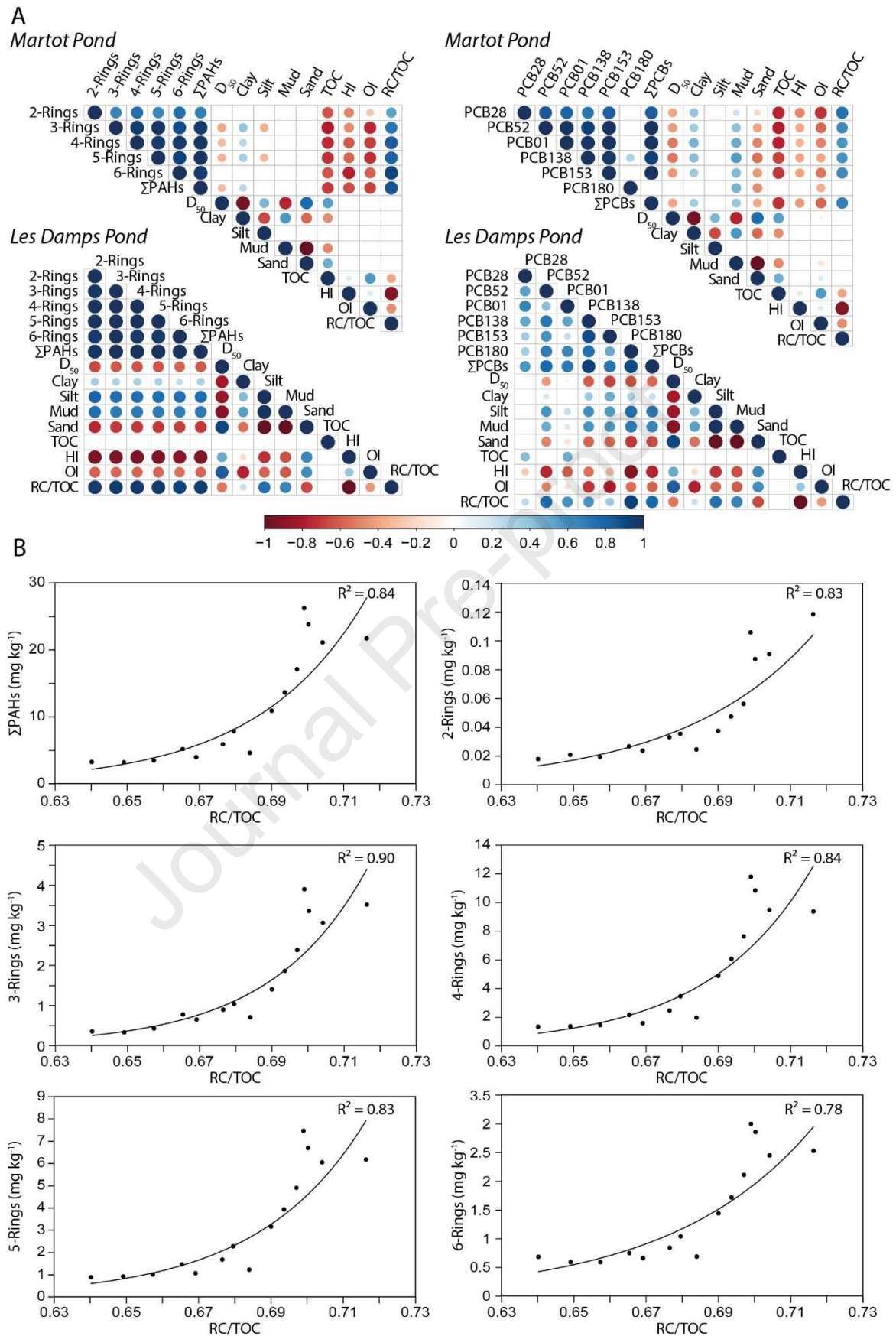


**Figure 3.** A. Correlation matrix of PAHs/PCBs and sediment characteristics for Martot and Les Damps ponds (Spearman correlation,  $p < 0.05$  for all circles presented); B.  $\Sigma$ PAHs, 2-3-Rings, 4-Rings, 5-Rings, and 6-Rings ( $\text{mg kg}^{-1}$ ) versus RC/TOC for Les Damps Pond (from the correlation matrix).

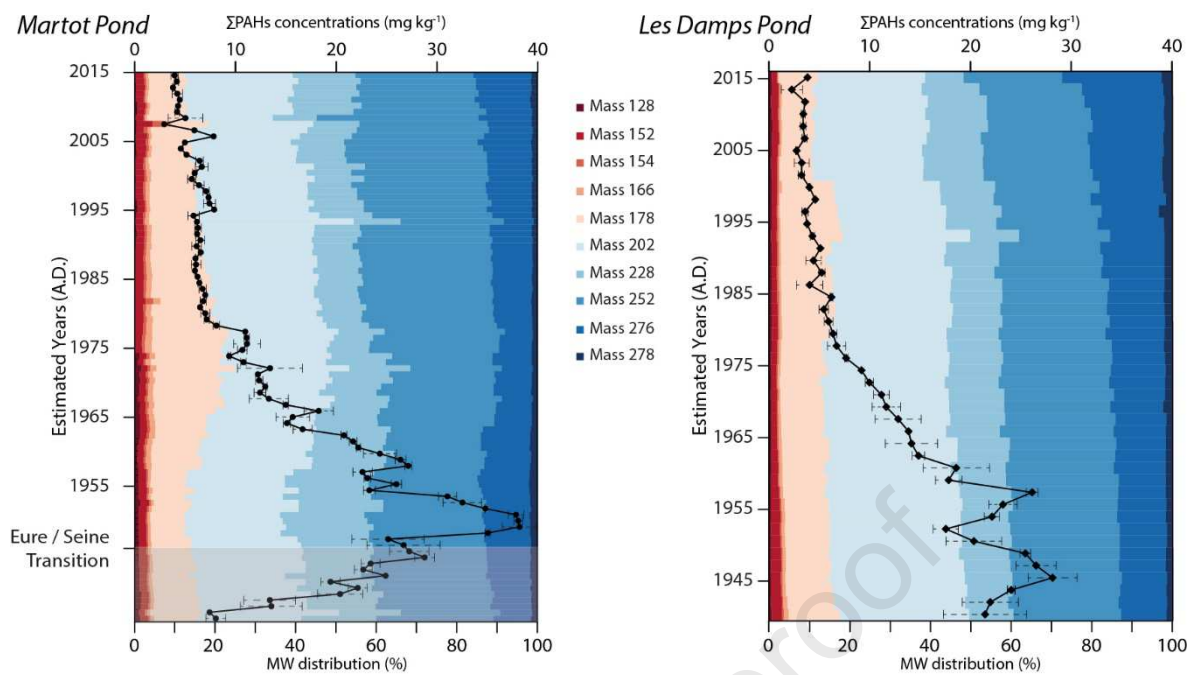


**Figure 4.** PAH concentrations ( $\text{mg kg}^{-1}$ ) and molar weight (MW) distribution (%) in Martot Pond (MAR16-02 core) and Damps Pond (DAM17-02 core).

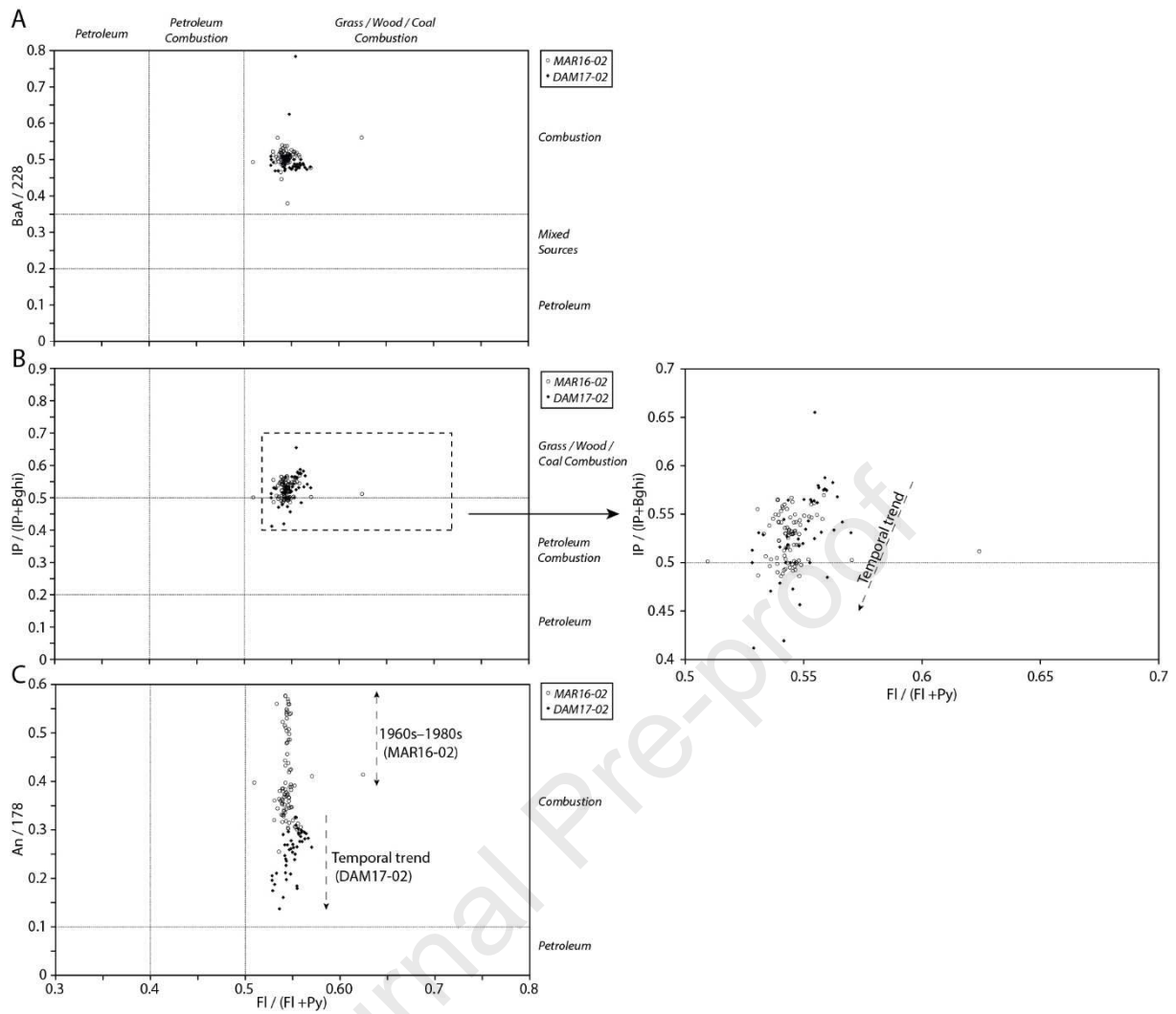


**Figure 5.** PAH diagnostic ratios A.  $BaA/228$  vs  $FI/(FI+Py)$ ; B.  $IP/(IP+Bghi)$  vs  $FI/(FI+Py)$  and C.  $An/178$  vs  $FI/(FI+Py)$  for the MAR16-02 (open circle) and DAM17-02 (black diamond) cores.

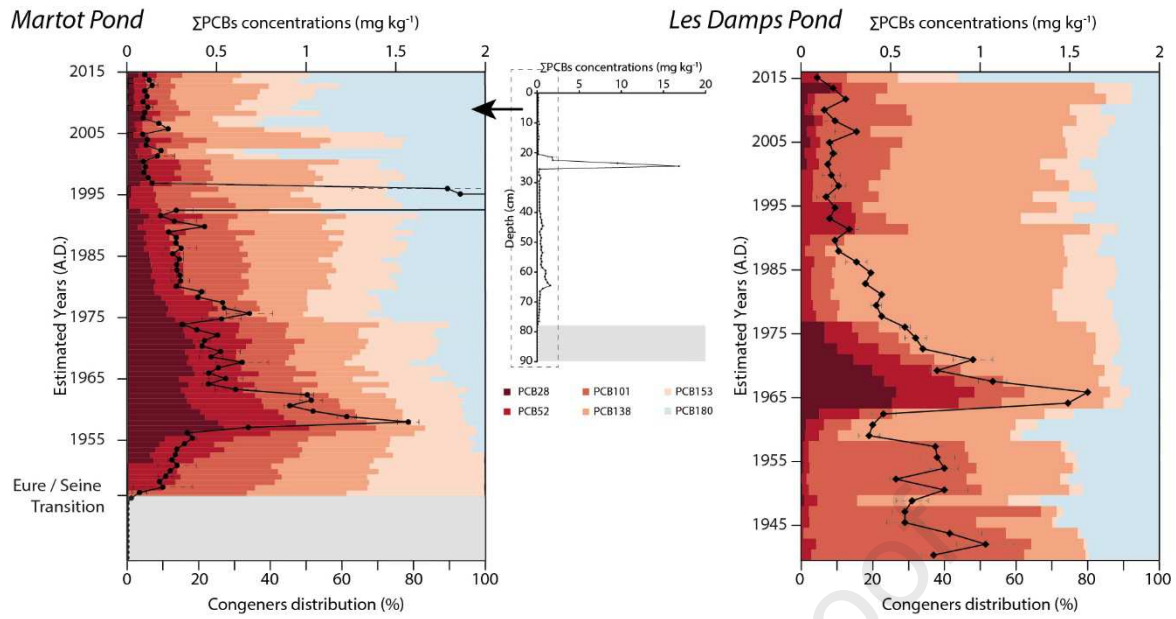


**Figure 6.** PCB concentrations and homolog distribution in Martot Pond (MAR16-02 core) and Les Damps Pond (DAM17-02 core).

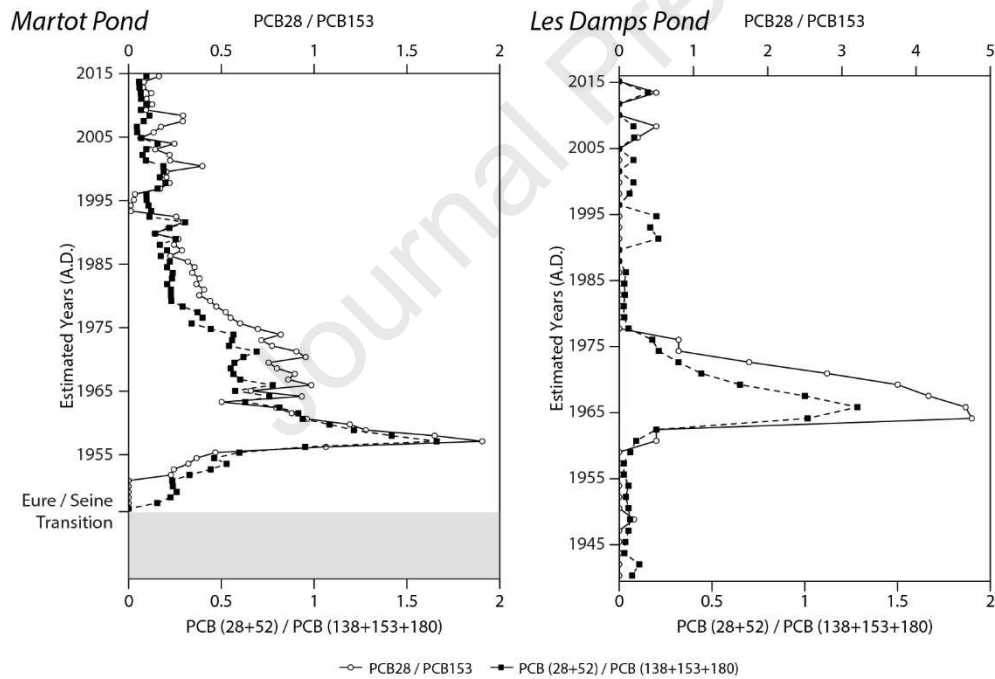


**Figure 7.** PCBs ratios in Martot Pond (MAR16-02 core) and Les Damps Pond (DAM17-02 core).

- Temporal trends of PAHs and PCBs were reconstructed from sediment cores
- PAHs and PCBs showed a positive correlation with fine fractions
- PAHs showed a positive correlation with the refractory organic carbon
- PAHs were found to be predominantly of pyrogenic origin
- High levels of PCBs were linked to technical mixture discharges into the river

Journal Pre-proof



**Declaration of interests**

The authors declare that they have no known competing financial interests or personal relationships that could have appeared to influence the work reported in this paper.

The authors declare the following financial interests/personal relationships which may be considered as potential competing interests:

Journal Pre-proof